Rodrigo Cortes dos Santos

Licenciado em Engenharia de Micro e Nanotecnologias

Copper nanowires for next generation transparent conductors

Dissertação para obtenção do Grau de Mestre em
Engenharia de Micro e Nanotecnologias

Orientador: Doutor Pedro Miguel Cândido Barquinha, Professor Auxiliar, Faculdade de Ciências e Tecnologia da Universidade Nova de Lisboa

Júri:

Presidente: Doutor Rodrigo Ferrão de Paiva Martins, Professor Catedrático, Faculdade de Ciências e Tecnologia da Universidade Nova de Lisboa

Arguente: Doutor Rui Alberto Garção Barreira do Nascimento Igreja, Professor Auxiliar, Faculdade de Ciências e Tecnologia da Universidade Nova de Lisboa

Vogal: Doutor Pedro Miguel Cândido Barquinha, Professor Auxiliar, Faculdade de Ciências e Tecnologia da Universidade Nova de Lisboa

Outubro 2016

FACULDADE DE
CIÊNCIAS E TECNOLOGIA
UNIVERSIDADE NOVA DE LISBOA

Copper nanowires for next generation transparent conductors

ACKNOWLEDGMENTS

ABSTRACT

In this work, copper nanowires (CuNWs) were synthesized for application in transparent conductors, as an exploratory work for the replacement of conventional indium-tin oxide (ITO) thin films. Two syntheses were made, one of them costing less than 4 € per synthesis. Numerous deposition methods were applied and several nanowire inks were used. The best ink was shown to be CuNWs with 7 wt% in isopropyl alcohol (IPA), and a newly developed method was designed to deposit NWs.

The ink of CuNWs was deposited on top of interdigitated electrodes on glass. CuNWs on electrodes with gaps of 5, 10 and 30 μm registered a resistance as low as 68.07, 25.81 and 71.84 Ω, respectively. The films deposited directly on glass with top electrodes revealed a high electrical resistance, presumably due to high contact resistance. Inefficient intra-network welding (i.e., between NWs) was also responsible for the trend of increased resistance with higher number of consecutive depositions. Manual pressing was applied to the films, however, this process peeled off some CuNWs due to the lack of surface adhesion. So, numerous surface treatments were applied to glass surfaces, but then the surface roughness did not allow for a perfect deposition of aluminium contacts by e-beam.

The optical properties of the films with different thicknesses (obtained with several subsequent depositions) were measured, with the optical transmittance decreasing for larger number of depositions. Best equilibrium in terms of electrical/optical properties was achieved with a single deposition, for which electrical resistance of 65 Ω (5 μm gap) and 90 % optical transmittance were obtained.

Keywords: Copper, nanowires, transparent conductors

RESUMO

Neste trabalho sintetizaram-se nanofios de cobre (CuNWs) para aplicar em condutores transparentes, como um trabalho exploratório para substituição de filmes convencionais de óxido de índio-estanho (ITO). Foram feitas duas sínteses, sendo que uma custa menos de 4 € por síntese. Testaram-se inúmeros métodos de deposição e utilizaram-se várias tintas de nanofios. Demonstrou-se que a melhor tinta consistia em CuNWs com 7 % (m/m) em álcool isopropílico (IPA), e um novo método de deposição de NWs foi desenvolvido.

A tinta de CuNWs foi depositada no topo de elétrodos interdigitais em vidro. Os CuNWs em elétrodos com espaçamentos de 5, 10 e 30 μm registaram resistências de 68.07, 25.81 e 71.84 Ω, respetivamente. Os filmes depositados diretamente no vidro revelaram uma elevada resistência elétrica, presumivelmente devido à elevada resistência de contacto. Uma ineficaz soldadura intra-rede (i.e, entre NWs) foi responsável pelo aumento da resistência com o incremento do número de deposições. Aplicou-se pressão manual nos filmes, contudo, este processo arrancou alguns CuNWs devido à sua baixa adesão à superfície. Por este motivo, aplicaram-se vários tratamentos de superfície aos substratos de vidro, no entanto a rugosidade não permitiu uma deposição perfeita de contactos de alumínio por canhão de eletrões.

Mediram-se as propriedades óticas dos filmes com diferentes espessuras (obtidas através de várias deposições), com a transmitância ótica a diminuir com o aumento do número de deposições. O melhor equilíbrio em termos de propriedades elétricas/óticas foi alcançado com uma única deposição, com a qual se conseguiu uma resistência elétrica de 65 Ω (5 μm de espaçamento) e uma transmitância ótica de 90 %.

Termos-chave: Cobre, nanofios, condutores transparentes

LIST OF ABBREVIATIONS

a.u.   – Arbitrary units

AgNW   – Silver nanowire

APTES   – (3-Aminopropyl)triethoxysilane

CENIMAT   – Centro de investigação de materiais

CNT   – Carbon nanotube

Cu   – Copper

CuNW   – Copper nanowire

EDA   – Ethylenediamine

EtOH   – Ethanol

FIB   – Focused ion beam

IPA   – Isopropyl alcohol

ITO   – Indium tin oxide

LED   – Light emitting diode

M_w – Molecular weight

NaOH   – Sodium hydroxide

NW   – Nanowire

OLED   – Organic light emitting diode

OPV   – Organic photovoltaic

PEDOT:PSS   – Poly(3,4-ethylenedioxythiophene):polystyrene sulfonate

PV   – Photovoltaic

PVP   – Polyvinylpyrrolidone

rpm   – Rotations per minute

SEM   – Scanning electron microscope

UV   – Ultraviolet

XRD   – X-ray diffraction

LIST OF SYMBOLS

R   – Electrical resistance

%T   – Optical transmittance

x

TABLE OF CONTENTS

LIST OF FIGURES

LIST OF TABLES

1. MOTIVATION AND OBJECTIVES

1.1. Motivation

In our modern society, transparent conductors mainly fabricated from indium tin oxide (ITO) are found in a plethora of electronic and optoelectronic devices [1]–[3]. Despite all the attractive features of ITO, the production of this material is starting to suffer the consequences of an extensive mining over the last years, which inflates its price [1][2][4][5]. Besides this, there is a current demand for future applications in electronics, involving low-cost materials and fabrication, and stretchable components. Altogether, these factors are driving forces for the search of reliable alternatives to ITO [2][3].

In order to meet these needs, and taking as a starting point the research already performed on nanowires (NWs), the study of copper nanowires (CuNWs) was established, to take advantage from copper's virtues relatively to other metals.

1.2. Objectives

The main objective of this work is to start a new branch of studies on the field of transparent conductor films. Therefore, the final goal is to create a transparent conductive film of CuNWs. To achieve this, the following aspects are essential:

- Study of the effects of the synthesis' parameters;
- Study of several deposition methods;
- Study of CuNWs' inks;
- Study of the films' electrical properties;
- Study of the films' optical properties.

2. INTRODUCTION

In our daily lives we are surrounded by devices in which the transparency of their conductors is a crucial factor, namely flat panel displays, organic light emitting diodes (OLEDs), photovoltaics (PVs), and touch sensors [1]–[3]. ITO is certainly a very popular ceramic material for the production of transparent conductors, which is attributable to its high transmittance and low sheet resistance [1][2]. Nonetheless, ITO is not free of drawbacks. Because of its ceramic nature, ITO is brittle and, therefore, prone to cracking, which prevents its use in flexible applications [6]–[8]. The scarcity of indium on earth, together with the difficulty in its recycling and the excessive demand of ITO, are additional disadvantages for the broad usage of this material [3]. In fact, the supply of indium was seriously affected by the stoppage of mining from some Chinese companies, which triggered the rise of indium's price [4][5]. All these factors inspired the search for ITO's replacements. Ideally a good replacement should be deposited faster than ITO and have an equal or better electronic and optical performance [7].

2.1. ITO's possible replacements

Several materials have been studied aiming the replacement of ITO, from polymers to carbon structures such as carbon nanotubes (CNTs) and graphene, but all of these failed to meet some of the requirements previously mentioned. The major disadvantage of polymers is their inability to stand high currents, a mandatory property in organic photovoltaics (OPVs), since the electrode has to extract charge carriers from the absorbing layer [7]. For CNTs, their optical transmittance is inferior to that of ITO at the same sheet resistance [9]. The production of graphene is a very expensive process in either energy and heavy machinery, since it is grown mainly by chemical vapor deposition at really high temperatures, 650-1000 ℃ [10]. Also, sheet resistance is yet to reach ITO's level of performance [11].

These studies stimulated the search for new options, which consequently put metals on the spotlight as promising candidates to replace ITO [12]. Metals can be characterized by some specific properties. Those properties are high electrical and thermal conductivity, as well as malleability, ductility, and high reflectivity of light [13]. In addition, when compared to the other materials, the high electrical conductivity of metals makes them the best electrical conductors [12]. The major handicap of metals is their low transparency. Even so, by transforming the metal films into a grid with open holes that allows light's transmission, their optical performance can be improved. Yet, the cost of such films will raise and these cannot be used in OPVs, neither in OLEDs, since they do not allow flexible applications [9].

Auspiciously metallic NWs appeared as a good alternative to metallic films or grids. Their production can be as simple as a solution phase synthesis, and a transparent film is easily obtained by coating on a transparent substrate. On one hand, noble metals such as silver and gold could be an option to produce NWs, since these materials in such shape display similar resistivity to their bulk counterparts. However, both metals are expensive [14]. On the other hand, copper is more abundant and cheaper than silver or indium, and its conductivity is only 6 % lower to that of silver [3][14][15].

Table 2.1 establishes the main differences between all previously referred materials.

Table 2.1 – Comparison between ITO and its possible replacement materials.

	Transmittance	Electrical conductivity	High currents	Solution coatable	Stretchable
ITO [1][2][6]–[8]	✓✓✓	✓✓✓	Yes	Yes	No
Polymers [7][16]	✓✓✓	✓✓✓	No	Yes	Yes
CNTs [9][16]	✓✓	✓	-	Yes	Yes
Graphene [10][16]	✓✓	✓	-	No	Yes
Metal films [9][12][13]	✓	✓✓✓	Yes	No	No
Metal grids [9]	✓✓	✓✓✓	Yes	No	No
Metal NWs [14]	✓✓✓	✓✓✓	Yes	Yes	Yes

2.2.   Copper and copper nanowires

Copper is mankind's oldest metal, dating back some 10 000 years. All the great civilizations of the past used copper and its alloys. Though, it was in the Industrial Revolution that copper and copper alloys faced a remarkable change in their way of production and consumption [17].

Since copper belongs to group 11 of the periodic table, this means it has certain attributes: it has one s-orbital electron on top of a filled d-electron shell and is characterized by high ductility and electrical conductivity. The filled d-shells in this element do not contribute much to the interatomic interactions, which are dominated by the s-electrons through metallic bonds. Unlike metals with incomplete d-shells, metallic bonds in copper are lacking a covalent character and are relatively weak. This explains the low hardness and high ductility of copper single crystals. Furthermore, copper alloys are widely used, because they have unique mechanical and physical properties in addition to excellent corrosion and wear resistance [18]. Given that a material can change its properties at nanoscale and be affected by quantum effects, there has been some discussion on whether CuNWs would have a similar resistivity compared to its bulk material [19].

CuNWs' conductivity is in conflict with their transmittance: when one increases, the other decreases [8]. A compromise between both phenomena must be reached. In a NW film, conduction is due to electrons percolation across a path of interconnected NWs. There are some important parameters to achieve percolation: NW's concentration, length, and homogeneity. Since the contact resistance is much higher than the resistance of a single NW, long NWs are much more desirable instead of a big density of NWs [9].

2.3.   Synthesis of copper nanowires

Several routes may be used to synthesize CuNWs. In the case of electrospinning and vapor deposition, the expensive machinery required for their execution and the difficulty in scaling up these techniques represent their major drawbacks. Chemical solution arises as a viable and popular alternative, having been adopted by numerous labs. The main approaches used are an ethylenediamine (EDA) mediated synthesis [2][5][20] and an alkylamine mediated synthesis [8][21][22]. A comparison between the results found in the main studies is shown in Figure 2.1.
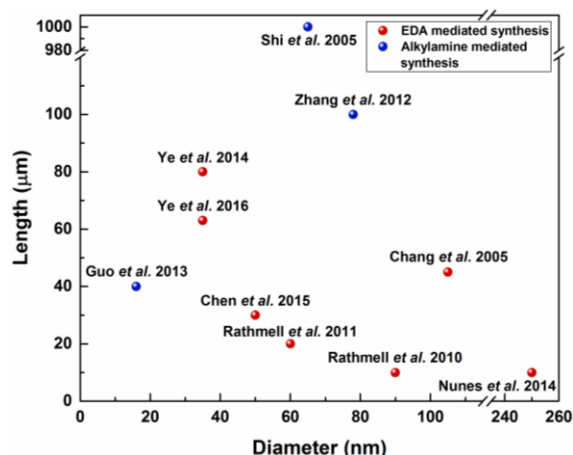
Figure 2.1 – Graphic showing some of the results obtained so far by other research groups. In Chang *et al.* [20] the average values were considered. Shi *et al.* [21] did not fully specify the CuNWs length and the diameter was an average of the results presented. Zhang *et al.* [22] also did not fully specify the CuNWs length [2][5][8][23]–[26].

Back in 2005, an EDA mediated synthesis was established by Chang and coworkers, in which EDA was added to the reaction to promote the anisotropic growth of Cu [20]. This solution phase synthesis showed CuNWs with 90-120 nm in diameter and lengths varying between 40-50 μm. Then, Rathmell *et al.* [5] proved that the previous reaction could be performed in a large-scale way by scaling it up by 200 times, which resulted in 1.2 g of CuNWs with an average diameter of 90 nm and 10 μm long. In the following year, the same group was able to further enhance the CuNWs dimensions to 60 nm and 20 μm. Such was accomplished by keeping the solution at 80 ℃ for 3 minutes, followed

by the addition of polyvinylpyrrolidone (PVP), which avoids the formation of aggregates, and letting the CuNWs grow in an ice bath [24]. Ye *et al.* [2] studied the effect of all parameters very deeply. They were able to rise the CuNWs' aspect ratio up to 2300. The resulting CuNWs had an average length of 80 μm, with some of those CuNWs reaching 200 μm, whereas the average diameter was 35 nm. Inspired by the previous reactions, Chen *et al.* [25] were able to obtain NWs with lengths between 20-30 μm and diameters of 50 nm. The main difference to the preceding reactions was the adding of the reagents in an ice bath. More recently, Ye *et al.* [23] decided to study the reaction kinetics and achieved CuNWs with 35 nm of diameter and 63 μm of length. At Centro de Investigação de Materiais (CENIMAT), Nunes *et al.*[26] achieved NWs with an average length of 10 μm and an average diameter of 250 nm, using copper acetate instead of copper nitrate in Chang's method [20].

Shi *et al.* [21] used an alkylamine mediated synthesis in which octadecylamine had a double function: to promote the reduction of copper ions and to work as a capping agent. The as-produced CuNWs were several millimeters long and displayed 30-100 nm in diameter. Zhang and coworkers [22] reported a nonaqueous synthesis of CuNWs by self-catalysis in which the CuNWs were grown in a tubular medium, created by the mixing of hexadeceylamine and cetyltriamoninum bromide. The research group also noted the need to use platinum, responsible for the catalysis of the copper ions' reduction. These CuNWs had lengths from tens to hundreds of micrometers and the diameter was ca. 78 nm. Guo *et al.* [8] used oleylamine instead of octadecylamine, and nickel ions (Ni^{2+}) as catalyst for copper reduction. The CuNWs had an aspect ratio of 2500, with lengths of 40 μm and an average diameter of 16 nm. In this synthesis, copper ions come from Copper (II) chloride dihydrate, and chloride ions lead to an anisotropic growth.

2.4.   Fabrication of copper nanowires films

One may choose amongst different deposition methods to produce transparent conductor films, such as drop casting [27]–[29], Meyer rod coating [2][15][24], spray coating [29]–[31], and vacuum filtration [5][8], as presented in Figure 2.2.
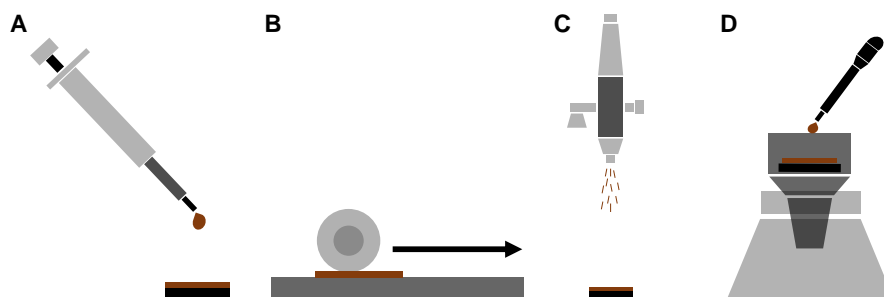
Figure 2.2 – Representation of drop casting A), Meyer rod coating B), spray coating C) and vacuum filtration D).

Drop casting is a simple technique in which a small volume of a solution with NWs is placed on top of the substrate and dried. Drying happens by solvent's evaporation with or without temperature [27]–[29]. Meyer rod coating comprises dragging a NWs' ink throughout the substrate with a Meyer rod. This is a very simple method, and lately the most common inks use nitrocellulose, which is very volatile and has a low evaporation temperature. So, it can be taken off with plasma cleaning and through heating in an oven [24]. More recently, Kang *et al.* [32] adapted the previous method and deposited NWs with polydimethylsiloxane nanochannels. The main goal of this new method is to produce films of aligned NWs. Spray coating consists of using an airbrush to deposit NWs. A solution with NWs is used and normally this technique requires a hot plate to evaporate the small drops, which are sprayed on the substrate. The drops size can be controlled by the pressure of the gas that flows inside the sprayer [29]–[31]. Vacuum filtration has some similarities with drop cast, however, the solvent is deposited on a filter membrane instead of being deposited on the final substrate. After vacuum, the NWs' film on the filter membrane will be transferred to the final substrate [8].

2.5. Reduction of the contact resistance between copper nanowires

CuNWs have a high tendency to oxidize in air, compared to bulk Cu, because the surface area is drastically increased. Such fact makes it more difficult to reduce the contact resistance. Nevertheless, protection from oxidation is discussed in Chapter 2.6.

The most common ways to reduce contact resistance are based on the exertion of a pressure on top of the NWs [11] and thermal annealing [33] (Figure 2.3 A and B).
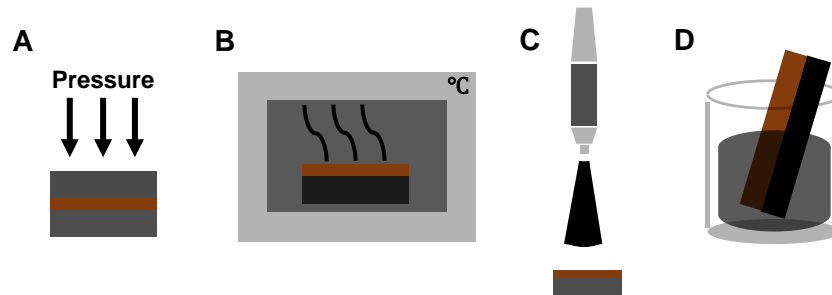
Figure 2.3 – Representation of some methods to reduce contact resistance. A) Mechanical pressure, B) thermal annealing, C) plasmonic laser welding and D) acid treatments.

Hu *et al.* [11] used two glass slides with a film of silver nanowires (AgNWs) between two metal plates. By pressing the metal plates through a mechanical manual pressure, the group was able to decrease the sheet resistance from hundreds to tens of Ω sq^{-1}, while the surface roughness was diminished as well. Thermal annealing at 200 ℃ for 20 minutes has been shown to significantly reduce the sheet resistance of a NWs' film [33]. However, annealing is not ideal because it requires temperatures above 100 ℃, which might induce oxidation of CuNWs.

Recently, researchers have been studying two new possibilities to counter oxidation: plasmonic laser welding [34], and acid treatments on the surface of CuNWs [35]. Han and co-workers [34] designed a plasmonic laser with fast scanning speed, which made possible the suppression of the oxidation problem during annealing of Cu. Acid treatments are able to remove the oxide from the CuNWs' surface and allow the possibility of integration in roll-to-roll processing.

2.6. Protection from oxidation

NWs require protection from atmospheric corrosion, given that CuNWs react with oxygen very easily and, as a consequence, they get more resistive.

Rathmell and co-workers [24] coated CuNWs films with a nitrocellulose-based ink in order to protect the NWs from oxidation. Afterwards the nitrocellulose was removed with plasma cleaner, leaving a highly conductive CuNWs network. The same researchers demonstrated a method for synthesizing CuNWs with nickel shells. Cupronickel NWs showed a higher resistivity than CuNWs. Also, since nickel covers copper, the diameters of the NWs increased to 200-300 nm. Despite this increase, which lowered the performance of the transparent conductive films, the sheet resistance increased by only 10 Ω sq^{-1} after 30 days [15]. More recently, CuNWs were coated with a metal, zinc, tin, or indium, by electroplating. This process was followed by oxidation to create oxides shells that protected the NWs, without degrading conductivity and transmittance of the films [3].

Han *et al.* [14] demonstrated a novel method to reverse copper oxidation through photothermochemical reduction. After the CuNWs are deposited in a film, they were oxidized by thermal oxidation. Ethylene glycol was posteriorly coated on top of the NWs, working as a reducing agent. Then the oxidized NWs were irradiated by a focused laser beam. The laser was generated by a diode-pumped solid-state Nd:YAG laser, because the wavelength is higher than copper oxides' bandgaps.

2.7. Highly stretchable and foldable electrodes

Various new materials have been studied to be used as stretchable and foldable electrodes, such as conducting polymers, CNTs, and graphene [16]. Nevertheless, they have shown limited applications and performance, because conductive polymers demonstrated poor stability and conductivity, and carbon-based nanomaterial revealed low electrical conductivity and high material cost [16]. To the author's knowledge there has not been much research on stretchable and foldable electrodes of CuNWs. Fortunately, Lee *et al.* made a breakthrough research with AgNWs, since they were able to get a highly stretchable and highly conductive NW percolation network. The network had a superior electrical conductivity and mechanical compliance compared to CNTs and graphene. To achieve such results the key factor was the NWs length [16].

2.8. Device Integration

Since markets for transparent conductors continue to grow and there is a demand for new materials, the next step for CuNWs is device integration. With that in mind, Sachse and co-workers [36] demonstrated a small-molecule organic solar cell with a transparent electrode of CuNWs. This cell revealed perfect electrical behavior with 3.1 % efficiency compared to 4.0 % for an ITO reference device. Then, Stewart *et al.* [35] used CuNWs, protected with nickel to prevent oxidation, as a conductor in an OPV. The device had an efficiency of 4.9 % compared to 7.1 % of ITO. The lower transmittance of the copper-nickel film could explain the lower efficiency of the device produced in the study. Later, Chen *et al.* [25] demonstrated an OPV with a contact of poly(3,4-ethylenedioxythiophene):polystyrene sulfonate (PEDOT:PSS), with CuNWs coated on it. This contact had a low surface roughness.

In light emitting diodes (LEDs), Guo *et al.* [8] showed perfect integration of CuNW networks in a GaN LED. The NWs transparent electrode had 90 % transmittance. However, it required an annealing at 200 ℃ for one hour to present good ohmic type characteristic. Nevertheless, this was still a promising result.

3. MATERIALS AND METHODS

3.1. Copper nanowires synthesis

Two syntheses were tested, one using copper acetate and another one with copper nitrate. Both methods produce NWs via chemical reaction.

3.1.1. Synthesis using copper acetate

NWs were produced following Nunes *et al.* [26] method. First, 24 g of sodium hydroxide (NaOH) was dissolved in 40 mL of water, raising water's temperature above 80 ℃. The solution was kept under stirring while 0.46 g of copper(II) acetate was dissolved in 20 mL of water. Then, after 15 minutes, 1.5 mL of copper acetate's solution was added to the NaOH solution in a dropwise manner, because the NaOH solution was still hot. Subsequently, 50 µL of EDA and 10 µL of hydrazine were also added to the previous solution. Afterwards, the solution was placed in a hot bath at 65 ℃ for one hour. This process is illustrated in Figure 3.1.
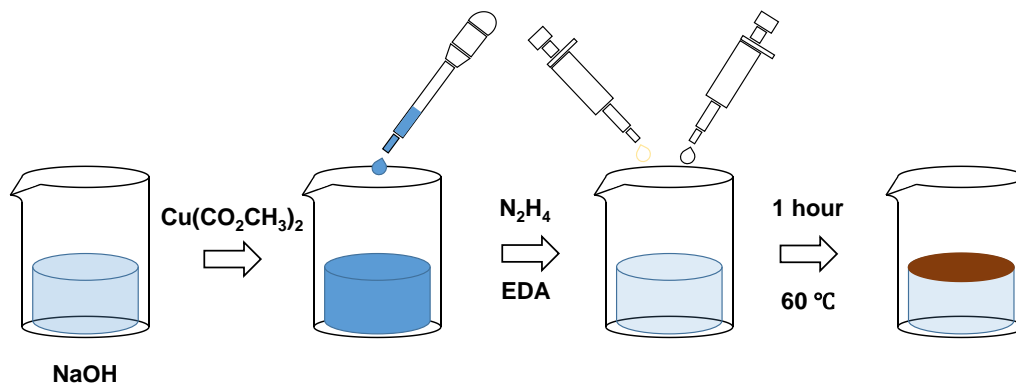
Figure 3.1 – Schematic of the reaction of CuNWs production troughout all the phases.

3.1.2. Synthesis using copper nitrate

This synthesis is based on a method developed by Rathmell *et al.* [5]. To start, 24 g of sodium hydroxide (NaOH) were dissolved in 40 mL of water and kept under constant stirring at 400 rpm. Another solution was prepared by dissolving 0.93 g of copper(II) nitrate hemi(pentahydrate) in 20 mL of water. After 10 minutes, 2 mL of this solution was added dropwise to the previous NaOH solution. Then, 600 µL of EDA and 50 µL of hydrazine (35 wt%) were added to the NaOH solution, and kept under stirring for 1 minute at 700 rpm. Subsequently, the solution was left in a hot bath at 80 ℃ for one hour (Figure 3.2).
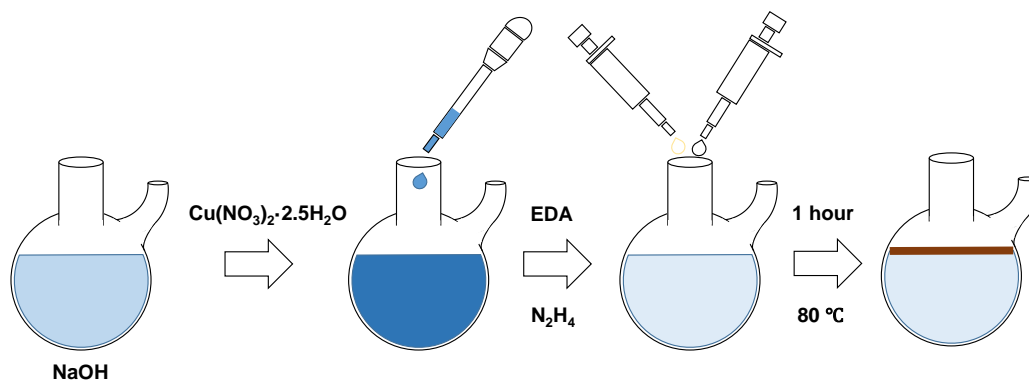
Figure 3.2 – Schematic of the CuNWs synthesis in all phases of the reaction.

3.1.3. Materials and reagents

NaOH was obtained from Fisher Scientific. Copper(II) acetate was acquired from Sigma-Aldrich. For the copper acetate reaction, EDA (99 %) was purchased from Merck. Copper(II) nitrate hemi(pentahydrate) and EDA (75-80 %) were purchased from Sigma-Aldrich. Both syntheses were made with the same hydrazine (65 wt%, Sigma-Aldrich), but for the copper nitrate synthesis, water was added to create hydrazine with 35 wt%. Deionized water (Millipore) was used.

3.1.4. Cleaning and dispersion of the nanowires

NWs were cleaned with isopropyl alcohol (IPA, Sigma-Aldrich) and deionized water (Millipore). Centrifugation was used in the cleaning process with runs of 5 minutes at 4000 rotations per minute (rpm), as illustrated in Figure 3.3 A.

Sonication was performed to NWs in IPA, in order to disperse them. The ultra-sonication was made with a cylindrical tip (3 mm end cap diameter) for 2 minutes in a UP400S sonicator, using an amplitude of 40 %. After sonication, the NWs were kept under stirring at 350 rpm, as demonstrated in Figure 3.3 B.
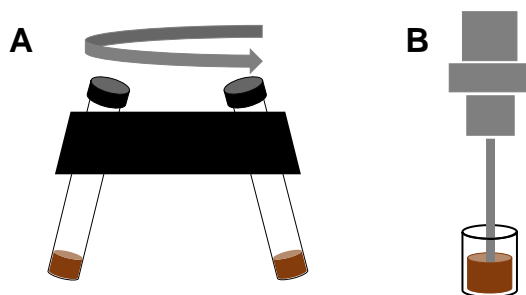
Figure 3.3 – Cleaning steps representation. A) represents centrifugation and B) sonication.

3.1.5. Characterization of copper nanowires: morphological and structural analysis

The morphological analysis of CuNWs was performed via scanning electron microscopy (SEM). The workstation was assembled by Carl Zeiss Auriga, and it is equipped with a Carl Zeiss Auriga crossbeam (SEM-FIB) and with an Oxford X-ray energy dispersive spectrometer. An optical microscope (Olympus BX51) equipped with an Olympus DP50 camera, followed by the Cell F View Image System Software, used to obtain images of the NWs, since they are long enough to be visible in the previous equipment. ImageJ software was used to determine the dimensions of the CuNWs from both SEM and optical microscope images.

Analysis of the CuNWs structure was carried by X-ray diffraction (XRD) using a PANalyticalX'Pert Pro X-ray diffractometer in Bragg–Brentano geometry, with a monochromatic Cu-Kα radiation source (wavelength 1.5406 Å). XRD measurements were carried out from 30° to 90º (2θ), with a scanning step size of 0.033°.

3.2.   Copper nanowires films

3.2.1. Materials and reagents

In drop cast a micropipette was used, as well as a hot plate and glass (VWR). Glass comes in squares of 10 cm × 10 cm and were cut in smaller pieces of 2 cm × 2 cm. Then the smaller glasses were cleaned in an ultrasounds' bath, first 15 mins in IPA, followed by 15 mins in acetone and finally 15 mins in water, the bath temperature was 60 ℃ for all. For spray coating the same type of glasses' 2 cm × 2 cm were used with the same cleaning process. In doctor blade the glasses used had 7 cm × 2 cm, while the interdigitated were bigger and thinner. Films were deposited by a film applicator from BYK, which supplements also came from BYK. The gold interdigitated contacts were

made by depositing photoresist on a glass, then exposing the photoresist to ultraviolet (UV) light, followed by photoresist's revelation. Afterwards, a thin layer of titanium was deposited by e-beam to create a good adhesion to Corning glass, followed by a deposition of gold, also by e-beam. Then the contacts were completed by lift-off.

To avoid aggregates during the study of NWs solutions, ethylene glycol (M_W = 62,07 g/mol) from Carlo Erba reagents was used, as well as ethanol (EtOH) absolute from Fisher Scientific, and PVP (M_W = 10 000 g/mol) from Sigma-Aldrich.

Silanization on glass was performed through two routes: chemical reaction and vacuum. To perform the chemical silanization, (3-aminopropyl)triethoxysilane (APTES) from Sigma-Aldrich was used, as well as EtOH absolute from Fisher Scientific. Three solutions were prepared with different weight percentage of APTES, and a glass was placed in a solution for ten minutes. Vacuum silanization was made by using trichloro(1*H*, 1*H*, 2*H*, 2*H*-perfluorooctyl)silane (97 %) from Sigma-Aldrich, with a vacuum pump from KNF Neuberger and a plastic desiccator. Glasses were placed in a vacuum container. Afterwards, three droplets of trichloro(1*H*, 1*H*, 2*H*, 2*H*-perfluorooctyl)silane were placed in a plastic Petri dish and the vacuum pump was kept on for 30 minutes. Then the vacuum pump was turned off and vacuum was maintained for three hours. UV-treatment was performed with NOVASCAN (PSD-UV) for one hour. The UV-light generated has two peaks, 185 nm and 254 nm.

3.2.2. Characterization of copper films: morphological, electrical and optical analysis

Films were morphologically analyzed by optical microscope (Olympus BX51) equipped with an Olympus DP50 camera, followed by the Cell F View Image System Software.

Electrical characterization was done by the two probes method, using Keysight B1500A with Cascade Microtech EPS150 at room temperature and in a dark room. The four probes method is more accurate, since each probe measures just one quantity, either voltage or current. Because the probes set to measure voltage have high input impedance, the current flowing through them is very low. However, applying the four probe method to the interdigitated is more complex.

Optical characterization was performed with a Perkin Elmer Lambda 950 UV-Vis-NIR Spectrophotometer. Measurements were performed between 250 nm and 2500 nm, with a step of 5 nm, by using the integrating sphere.

3.2.3. Contact angles measurement

Contact angles were measured with Contact Angle System OCA 15 and analyzed with Dataphyiscs-SCA 20, by Sessile drop-method. A droplet of water with 1 mL was used.

4. RESULTS AND DISCUSSION

4.1. Copper nanowires synthesis

Firstly, CuNWs were produced using copper acetate, since they were previously used in CENIMAT, however this synthesis wasn't study very deeply. More recently, a new synthesis was designed using copper nitrate.

4.1.1. Synthesis using copper acetate

In order to study the variation of the aspect ratio (length/diameter), three parameters were tested, namely hydrazine, EDA, and time. In these syntheses EDA works as a capping agent and hydrazine as a reducing agent. Since EDA is the capping agent, an augment of EDA should promote thinner NWs. Increasing the amount of hydrazine leads to an increase of CuNWs' diameter. This can lead to less resistive NWs, however their optical properties will be worse. The first reaction (Reaction A, Figure 4.1 A) was conducted as shown in Chapter Methods. The NWs produced showed a cylindrical shape and had an average diameter of 256 nm. Then another reaction was produced, this time with 15 μL of hydrazine (Reaction B), while the other parameters were maintained. The increase of hydrazine (5 μL more than Reaction A) led to the formation of NWs with greater thickness (272 nm). Furthermore, these NWs exhibited some clusters, as shown in Figure 4.1 B. Therefore, the NWs did not present the desired results and were not analyzed further ahead.

Afterwards, an alternative reaction was prepared, only varying the amount of EDA (Reaction C, Figure 4.1 C). The quantity of EDA added was 100 μL (doubling the quantity comparatively to Reaction A). The resulting NWs were thinner compared to those from first reaction, albeit some tapered effect was noticed. In the last attempt to maximize the CuNWs aspect ratio, the synthesis' duration was increased by one hour, resulting in a two hours long reaction (Reaction D, Figure 4.1 D).
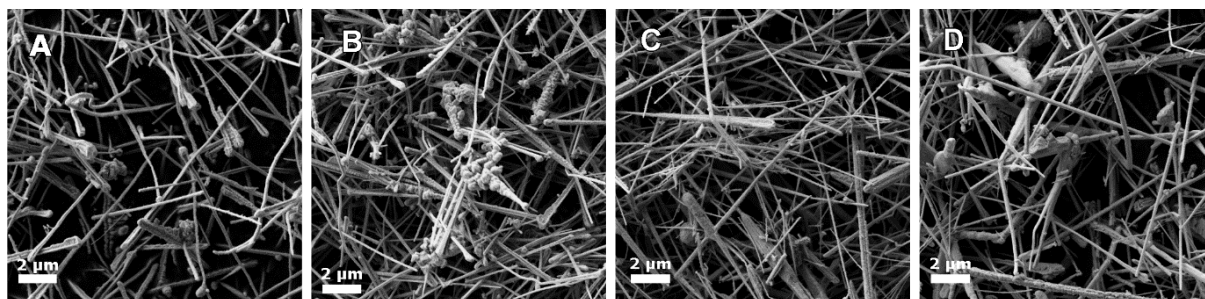
Figure 4.1 – Scanning electron microscopy image of the obtained CuNWs from reaction A (A), B (B), C (C) and D (D).

The study of the NWs' diameters is represented in Figure 4.2. Through the addition of more EDA to the solution, a reduction of more than 70 nm in the average diameter of the NWs was achievable, while keeping the standard deviation. Albeit, there are few NWs with more than 800 nm of diameter and, as mention before, a tapered effect was observable. When the reaction took one extra hour, the average diameter of the NWs was very similar. In fact, in the measured NWs, this parameter was decreased. This demonstrates one of the disadvantages from chemical synthesis: the NWs lack some control, so the results will always have a certain variation.
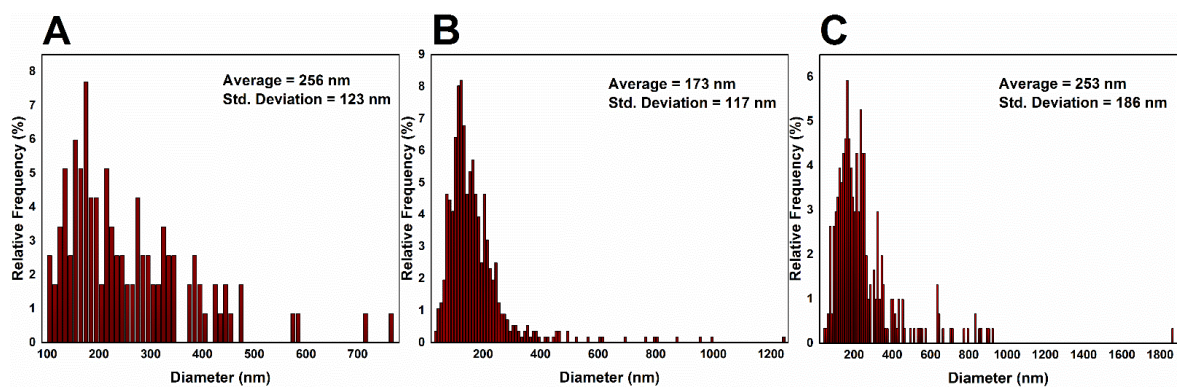
Figure 4.2 – Statistical study performed on CuNWs in order to optimize their diameter. A) shows reaction A, B) the reaction with 100 µL of EDA and C) the two hours long reaction.

Then the length of the NWs was studied (Figure 4.3) and again the results for the two hours long reaction are unexpected, showing there is no improvement in the CuNWs' average length for longer reactions. The reaction with more EDA exhibited an improvement in the CuNWs average length. Nonetheless, the standard deviation also increased.
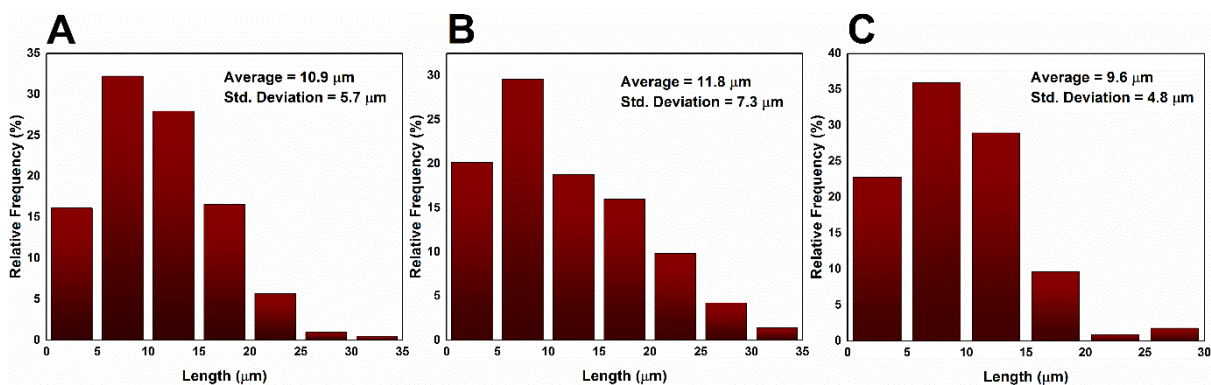
Figure 4.3 - Statistical study performed on CuNWs in order to optimize their length. A) shows reaction A, B) the reaction with 100 µL of EDA, and C) the two hours long reaction.

CuNWs formed from reaction A achieved an aspect ratio of 43, which was increased to 68 with reaction B since the length of the NWs increased and the correspondent diameters decreased.

The XRD patterns of CuNWs shown in Figure 4.4 exhibited a big presence of copper (111) plane in all three reactions (ICDD File: 00-004-0836). CuO's (111) plane (ICDD File: 01-080-1917) is present as well, and reaction D also had some evidence of Cu_2O's (111) plane (ICDD File: 01-077-0199).
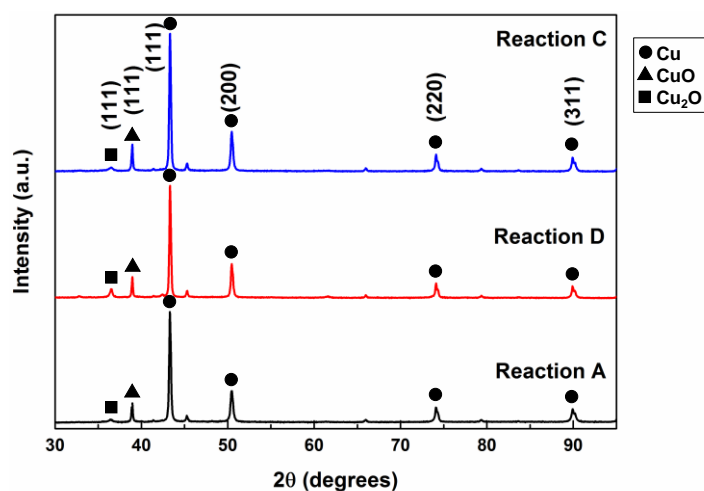
Figure 4.4 – Structural characterization of CuNWs for reactions A, C and D.

Increasing the amount of EDA added to the solution reduced the NWs diameter and increased their lengths, leading to an increase of the aspect ratio, which according to literature, will reduce their resistance. Nevertheless, the relative frequency for sizes between 0 µm and 5 µm for about 5 %, as well as the presence of CuO's (111), also increased, and oxidation is very undesired in CuNWs. Copper itself has already a strong capability to oxidize, so, since the increased sizes of the NWs was not very vast, we decided to take a conservative way and use the NWs from reaction A.

4.1.2. Synthesis using copper nitrate

NWs were produced as described in Chapter Methods. In this synthesis, a supernatant is formed after 15 minutes when the solution is left at the water bath. Having this in mind, some NWs were collected after 20, 30 and 60 minutes, to understand if the synthesis time could be lowered.
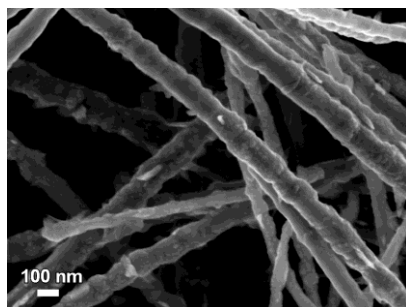
Figure 4.5 – Scanning electron microscopy image of CuNWs after 20 minutes.

Figure 4.5 shows that NWs are suffering some nucleation, which means they are still maturing.
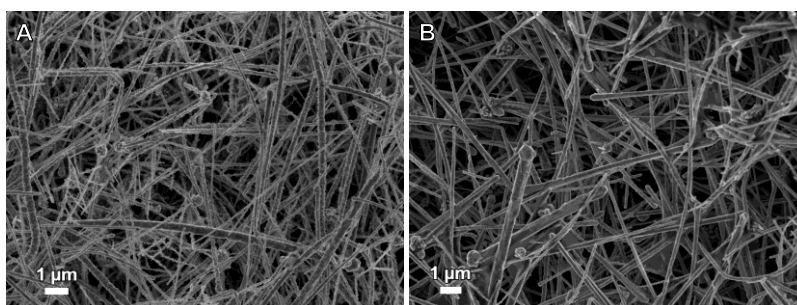
Figure 4.6 – Scanning electron microscopy image of CuNWs after 30 minutes (A) and 60 minutes (B).

NWs appear to exhibit smaller diameters in Figure 4.6 A in comparison to Figure 4.6 B. However, some nucleation was still found after 30 minutes as shown in Figure 4.7.
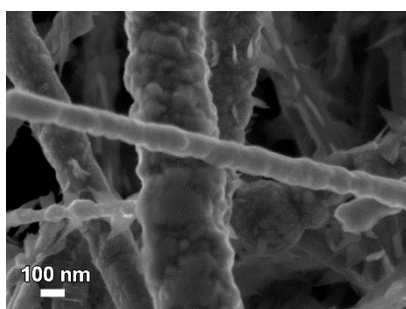
Figure 4.7 – Scanning electron microscopy image of CuNWs after 30 minutes, where some undergoing nucleation is visible.

Posteriorly, a statistical study was performed to the NWs produced with 30 minutes and 60 minutes of water bath, to fully understand how long the water bath should be to get optimal CuNWs.
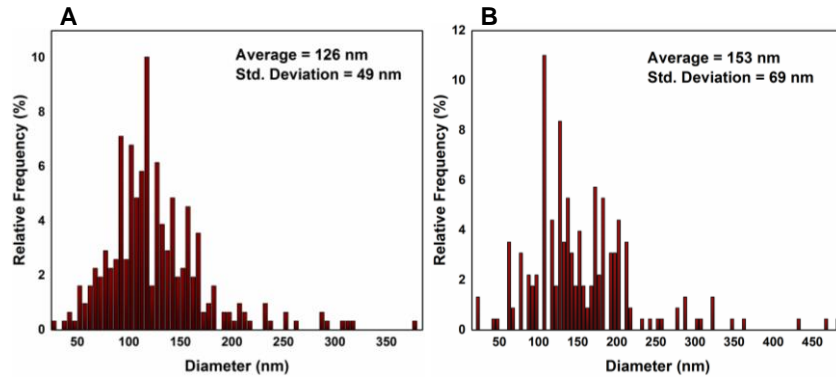
Figure 4.8 – Statistical study performed on CuNWs in order to optimize their diameter. A) shows the 30 minutes and B) the 60 minutes long water bath.

Indeed, longer water bath times increase the average diameter of the CuNWs (Figure 4.8), however, they also increased the NWs length (Figure 4.9), with some NWS achieving lengths of more than 60 µm.
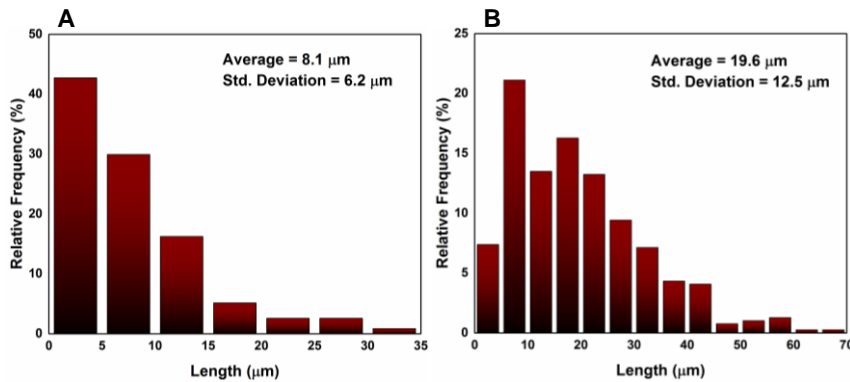
Figure 4.9 – Statistical study performed on CuNWs in order to optimize their length. A) shows the 30 minutes and B) the 60 minutes long water bath.

Afterwards, a structural characterization of the CuNWs with 60 minutes long water bath was performed. The same characterization was not performed to the other NWs, because the increased length of the NWs with 60 minutes long water bath is so great that makes the other CuNWs, with shorter water baths, unviable to use.
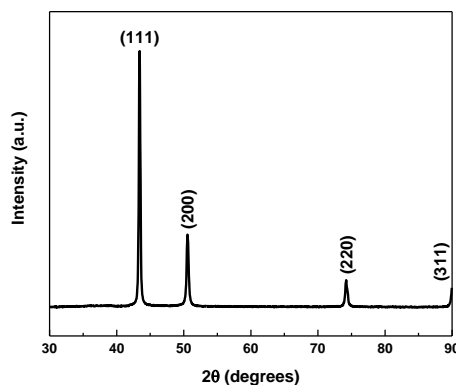
Figure 4.10 – Structural characterization of CuNWs.

XRD pattern of the CuNWs shown in Figure 4.10 only displayed the presence of copper planes (ICDD File: 00-004-0836).

These results are superior to the results obtained in the synthesis with copper acetate, since the aspect ratio was increased to 128. However, this new synthesis took some time to be fully functional and could not be tested electrically and optically.

4.2. Deposition methods

With the intention of getting a film of NWs deposited on glass, several deposition methods were tested. These methods were: drop casting, spray coating, and doctor blade. In all the methods the NWs used were with copper acetate.

4.2.1. Drop Casting

A starting test consisting of three experiments was carried with the conditions showed in Table 4.1. The NWs were stored in IPA and since IPA has a low boiling point (82.6 ℃), no temperature was used to evaporate it. An experiment schematic can be found in Annex A.

Table 4.1 – Parameters of the first drop casting experiment.

Experiment	Number of drops	Drop volume (µL)
1	10	10
2	10	5
3	10	20

The results of the test can be seen in Figure 4.11. The area of the NWs' film deposited is dependent on the drop quantity, so the smaller the drop quantity the smaller the area occupied by NWs. Interestingly, the first drop will spread more than its predecessors. Moreover, the drops after the first one will clean some NWs deposited on the center of the film to the drop boundary. This leads to the creation of some "rings", where the agglomeration of NWs is much denser compared to the average of the film.
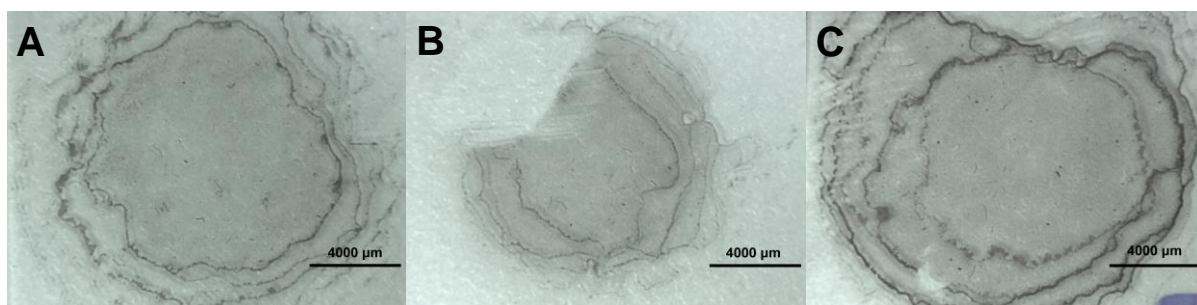
Figure 4.11 - Photographs from experiments 1 (A), 2 (B) and 3 (C).

In an attempt to control the area of the droplet spread, two possibilities were taken into account. One possibility was limiting the glass, so that the drop would not be free to spread, and the other one was adding temperature to promote a faster evaporation of IPA.

Four pieces of adhesive tape were placed on top of a glass leaving a square in the middle, then six drops of 5 µL of NWs solution were deposited. As seen in Figure 4.12 A, the main objective of this try was not reached, since there was a poor spread of the droplets. Due to the tape thickness, roughly 35 µm, when two pieces are overlapping it creates a space where the drop is free to move. It was also noticeable that tape presented a weird effect at the edges, since there is a sudden raise of height, and the effect of barrier is lost (Figure 4.13). Furthermore, the CuNWs were poorly dispersed and started to form some aggregates (Figure 4.12 B).
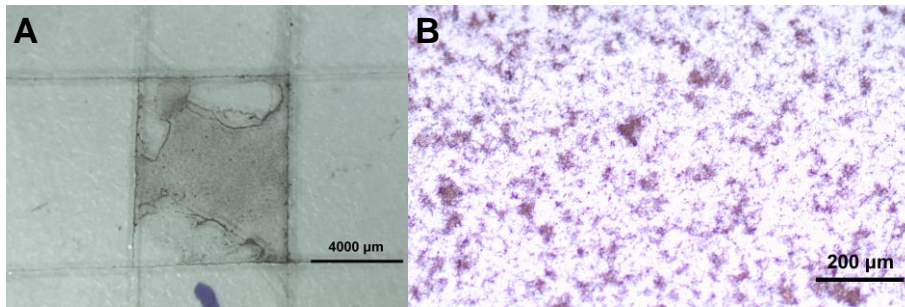
Figure 4.12 – A) Photograph from the results obtained when using tape. B) Microscopic image of the film.
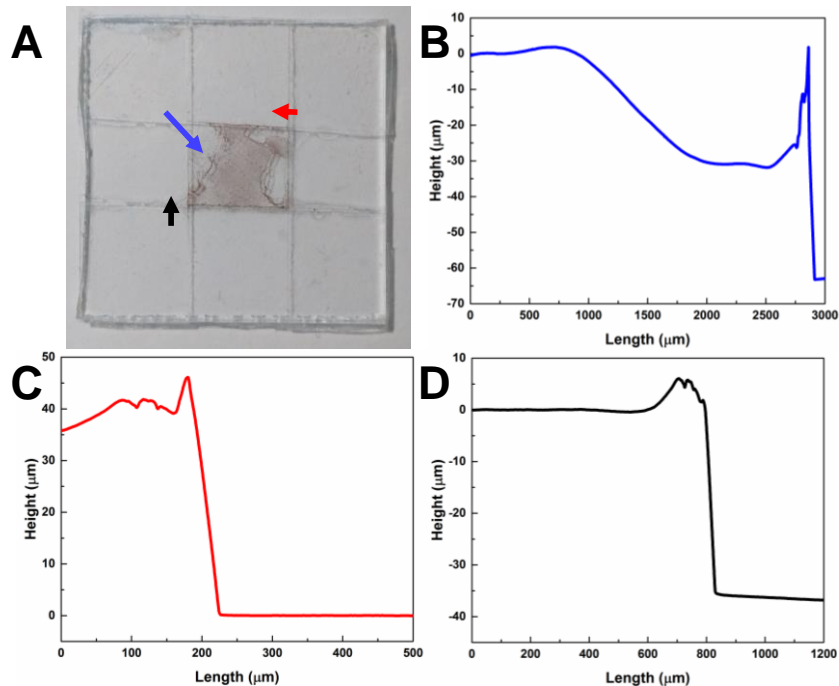
Figure 4.13 – A) Photograph of the sample with tape, where the arrows indicate the position and the direction of the profilometer measurement on the substrate. B), C) and D) are plots of the profilometer measurements of the respectives arrows.

Afterwards, the effect of the temperature was tested. The selected temperature was 40 ℃ because a higher temperature will evaporate IPA very fast, and the NWs will be dispersed in an undesired pattern (Table 4.2).

Table 4.2 – Parameters used on experiments 5 and 6.

Experiment	Number of drops	Drop volume (µL)
5	10	10
6	10	5

Comparing the first experiment to the fifth experiment, the NWs solution was visibly spread very easily on top of glass for both experiments. However, in the fifth experiment there is a small circle in the middle of the glass with higher transparency (Figure 4.14 A).
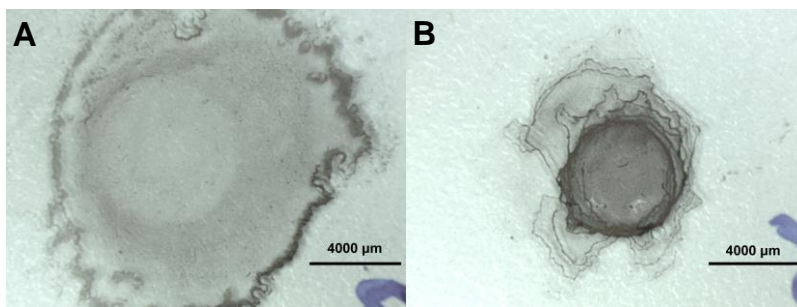
Figure 4.14 – Photographs from experiments 5 (A) and 6 (B).

Lowering the drop volume generated a much darker and small film, although the "coffee ring" effect was still present (Figure 4.14 B).

4.2.2. Spray coating

A small test was conducted aiming to check the viability of spray coating in terms of reproducibility and control. The spray gun pressure was set to 15 psi with N_2 gas, the distance between the glass substrate and the gun was 10 cm, and the substrate was under constant heating at 60 ℃.
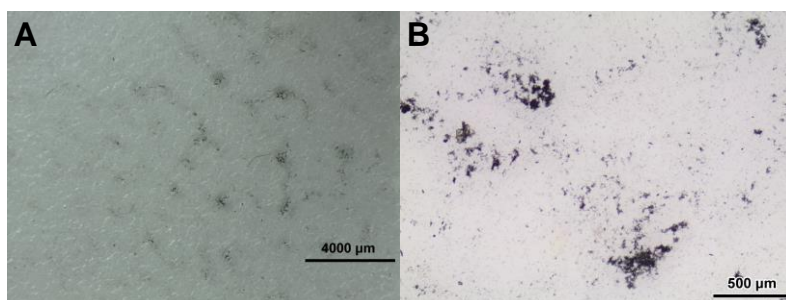
Figure 4.15 – A) Photograph of the film deposited by spray coating. B) Optical microscopy image from the same film.

The deposition by spray coating had no uniformity and created a lot of aggregates (Figure 4.15). To increase the film's uniformity, the sprayer would require some circulatory movements, in order to spray the NWs all along the surface. However, there is no machinery available in the lab to perform those movements. The same can be made by hand, but that will add the human error. So this deposition method was abandoned.

4.2.3. Doctor blade

To perform doctor blade a Meyer rod was used to spread the NWs on top of a glass substrate, which was seven centimeters length and two centimeters height (Annex B). The CuNWs were dispersed in IPA, in a concentration of 1 mg/mL, and the bar moved at a speed of 50 mm/s. Previously to the deposition, a UV treatment was carried on top of the glass substrate during 15 mins, followed by several depositions done in that glass substrate to understand how this can influence the number of CuNWs deposited.

Avoiding aggregates is essential to reach low transparency. In other words, a good dispersity of the NWs could lead to better transparent conductors. Having this in mind, higher viscosity solutions were considered as probable improvers of dispersity. Three parameters were varied, the number of depositions in the same substrate, drop quantity, and storing solution (Table 4.3).

Table 4.3 – Parameters varied on doctor blade performed with Meyer rod.

Solution	Number of depositions	Drop quantity (µL)
IPA + PVP (2 wt%)	1	25
	2	25
	1	10
	4	10
IPA + ethylene glycol (2 wt%)	1	25
	2	25
	1	10
	4	10

From all the results obtained, the ones shown ahead in Figure 4.16 were the best and all of them were made with drops of 10 µL. Additionally, the best storing solution was IPA with ethylene glycol (2 wt%). When the NWs were used in a solution of IPA with PVP (2 wt%), some aggregates were generated even with just one deposition. Also, the presence of PVP is noticeable around the NWs, so a further process would be needed to clean it, the most common being plasma treatment.
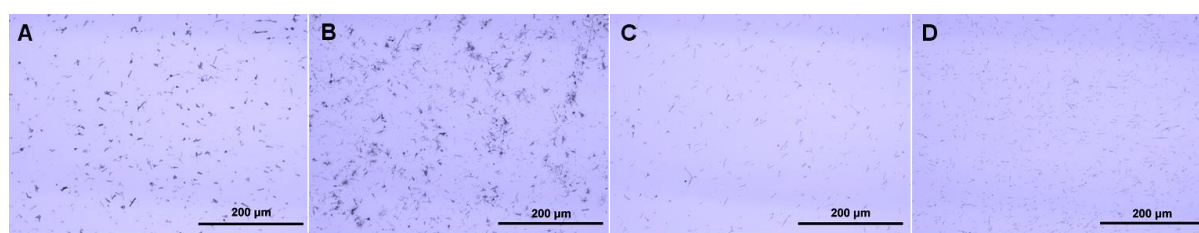
Figure 4.16 – Optical microscopy images from the results obtained with drops of 10 µL. In A) and B) the NWs were dispersed in IPA plus PVP (2 wt%), A) had one deposition and B) four depositions. In C) and D) the NWs were dispersed in IPA plus ethylene glycol (2 wt%), C) had one deposition and D) four depositions.

Subsequently a new solution was tried, using the former solution of IPA with PVP (2 wt%) to create a solution with 50 wt% water and 50 wt% IPA with PVP. Yet, like the solution without water, this one also generated some aggregates, which were visible after one deposition, as shown in Figure 4.17.
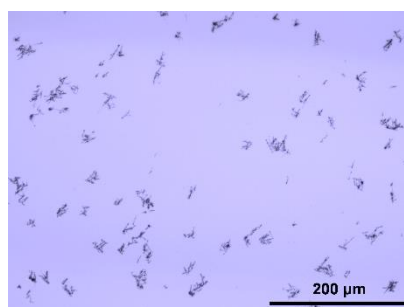
Figure 4.17 – Optical microscopy image of the result obtained with a solution of 50 wt% water and 50 % IPA with PVP.

At this point the use of UV treatment was questioned, and a further test was conducted by using the previous IPA with ethylene glycol (2 wt%) solution and a drop volume of 10 µL. After two depositions, the amount of NWs was visibly augmented, as seen in Figure 4.18 in comparison to the previous Figure 4.16 D), which had two more depositions. However, some of the previous effect that was shown by using PVP also occurred this time. There was some substance covering the NWs, which might be ethylene glycol.
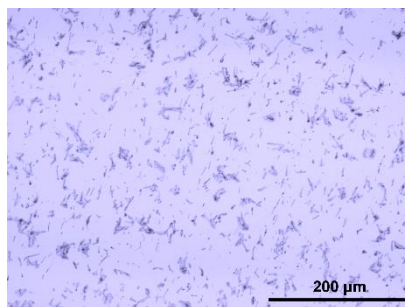
Figure 4.18 – Optical microscopy image of the result obtained with a solution of IPA with ethylene glycol (2 wt%).

Nevertheless, to obtain a conductor, several NWs would need to be in touch, and looking back at the results, even with four depositions on the same substrate, this goal was far from reachable. So, by switching the main focus from transparency to conductivity, a new method was verified. This new method uses one of the supplements for doctor blade. A piece of glass was taped to the back of the supplement, but just on top, letting the bottom of the glass to move freely, as shown in Annex C.

A comparison study between the Meyer rod and this new method was conducted, by using a solution of NWs in IPA with the same 1 mg/mL concentration, a drop volume of 10 µL, and without UV treatment.

Figure 4.19 – Photograph showing the difference between Meyer rod (top glass) and newly designed method (bottom glass).

In Figure 4.19, the difference between the two methods after five depositions is shown, the reddish color is more present in the glass where the newly designed method was used. Afterwards, the solution's concentration was increased to 7 mg/mL and a new film was deposited, again using the same conditions as before (Figure 4.20).
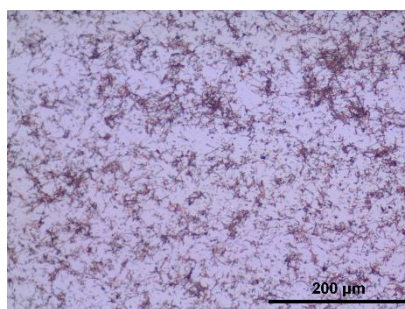
Figure 4.20 – Optical microscopy image of the result obtained with a NWs solution concentration of 7 mg/mL.

This effort exhibits the best results so far and the deposited film could be conductive, because it shows that a few CuNWs are creating a path.

4.2.3.1. Electrical characterization

Several samples were prepared to check the electrical performance of the CuNWs, varying the distance between the contacts. First, a film of CuNWs was deposited on top of some interdigitated

21

contacts. The schematic of the interdigitated contacts can be seen in Annex D. The interdigitated contacts had a length (*L*) of 4.2 mm, while the width (*W*) and the space between electrodes (*S*) were equal. The interdigitated with gaps of 5 μm have 300 contacts, the 10 μm have 150, 30 μm possess 50, and finally the 50 μm hold 30 contacts. In all the depositions, it was assured that the solution spread through all the contacts. Then a film of CuNWs was deposited on glass, first with bottom contacts, afterwards with top contacts.

4.2.3.1.1. Nanowires on interdigitated contacts

Using the same parameters as stated before, of five depositions with a highly concentrated solution (7 mg/mL), drop volume of 10 μL, and a deposition speed of 50 mm/s, a conductive path was generated on the 5 μm and 10 μm separated interdigitated contacts. Among the 30 μm and 50 μm interdigitated contacts there was no conductive channel as the results in Figure 4.21 suggest.
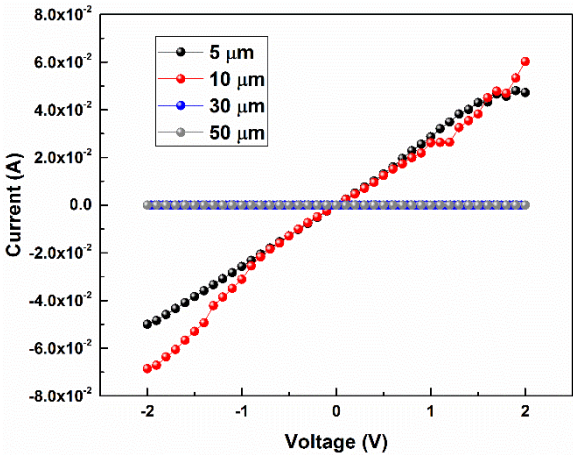
Figure 4.21 – Graphic of the IV curvers obtained for four interdigitated gaps.

The interdigitated contact with 5 μm showed a very linear performance right away, as a typical behavior expected for a conductor, having a resistance of 37.75 Ω.

All the interdigitated contacts with 10 μm were functional, although they did not exhibit a fully ohmic behavior. This could be due to contact resistance, between NWs and between the NWs and the contact itself. So the Meyer rod was used throughout the sample just to apply pressure on the NWs and after another electrical measurement, the NWs displayed an ohmic behavior (Figure 4.22).
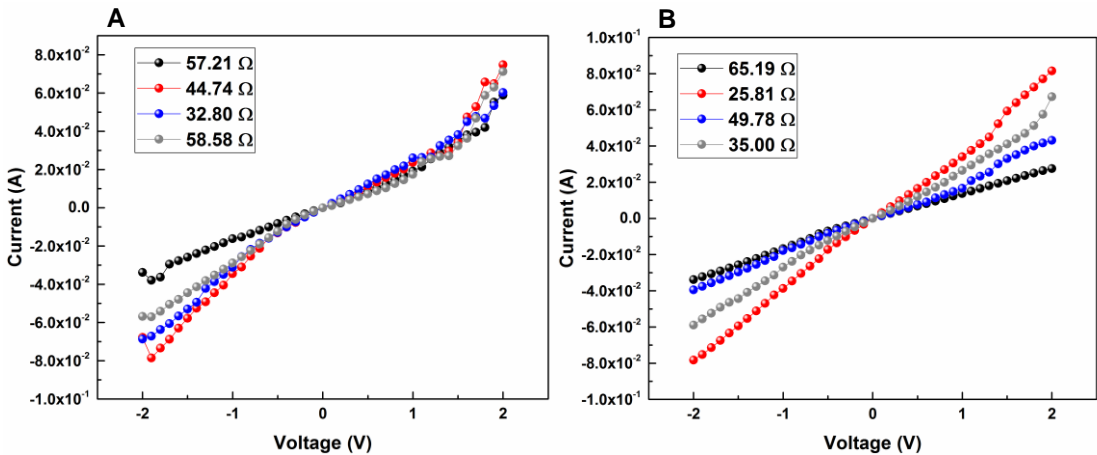
Figure 4.22 – Graphic of the IV curve before pressure (A) and after applying pressure (B).

The resistance was calculated by Ohm's law, and although some contacts dropped in resistance, others increased, which makes it impossible to find a correlation between pressure and resistance. Another interesting effect is shown in Figure 4.23. In the first voltage sweep, the calculated resistance was 65.20 Ω. However, in the last voltage sweep, the resistance decreased to 30.62 Ω,

inducing the presence of an activation energy. Throughout the voltage sweep, the absence of NWs' hysteresis is notorious, which is the expected behavior of a conductor.
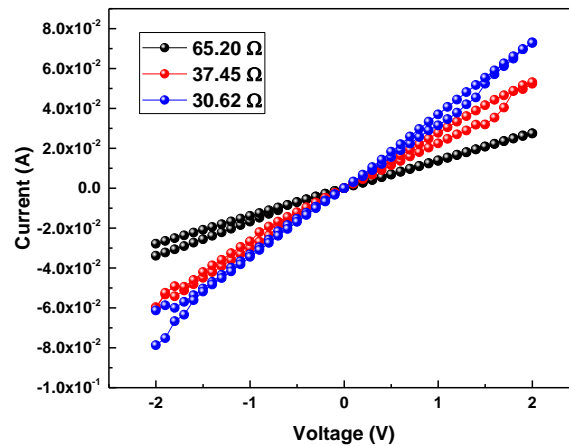
Figure 4.23 – Graphic of the IV curves performed in the same contact.

The Meyer rod was also used on the contacts with 30 µm. Having in mind that NWs might need some activation energy, and after some measurements in which they were not conducting, a voltage sweep between -40 V and 40 V was applied to the contacts, which made the NWs' film conductive (Figure 4.24).
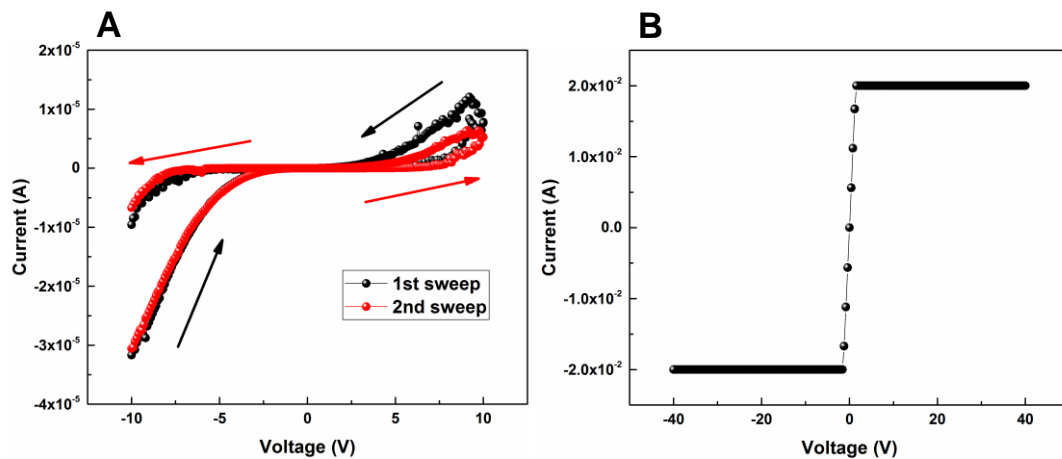
Figure 4.24 – A) IV curves of the first two sweeps aplied to the interdigitated contact with 30 µm gap. B) IV curve of the voltage sweep between -40 V and 40 V with compliance set to 20 mA.

At this point a new sweep was done to analyse the resistance of the contact, consisting in a voltage sweep between -1 V and 1 V. The curve shows a perfectly ohmic behaviour and a resistance of 71.89 Ω, which is slightly higher compared to the interdigitated contacts with less gap (Figure 4.25).
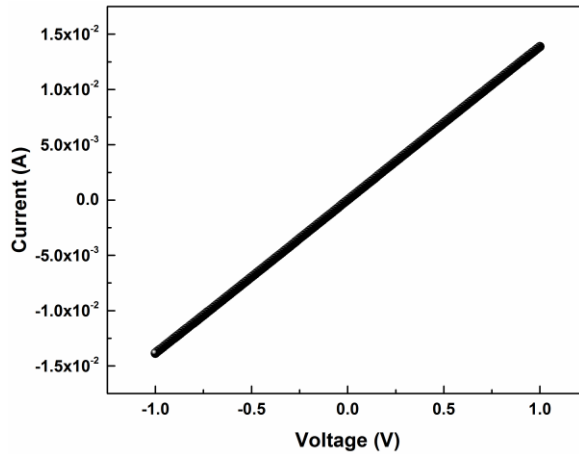
Figure 4.25 – IV curve done to the contact with 30 μm gap from -1 V to 1 V.

After this, a new study was conducted to check the contacts performance throughout the depositions. Five depositions were done on the contacts with gaps between 5 μm, 10 μm and 30 μm, and a final passage with the Meyer rod was performed to apply pressure on the NWs.
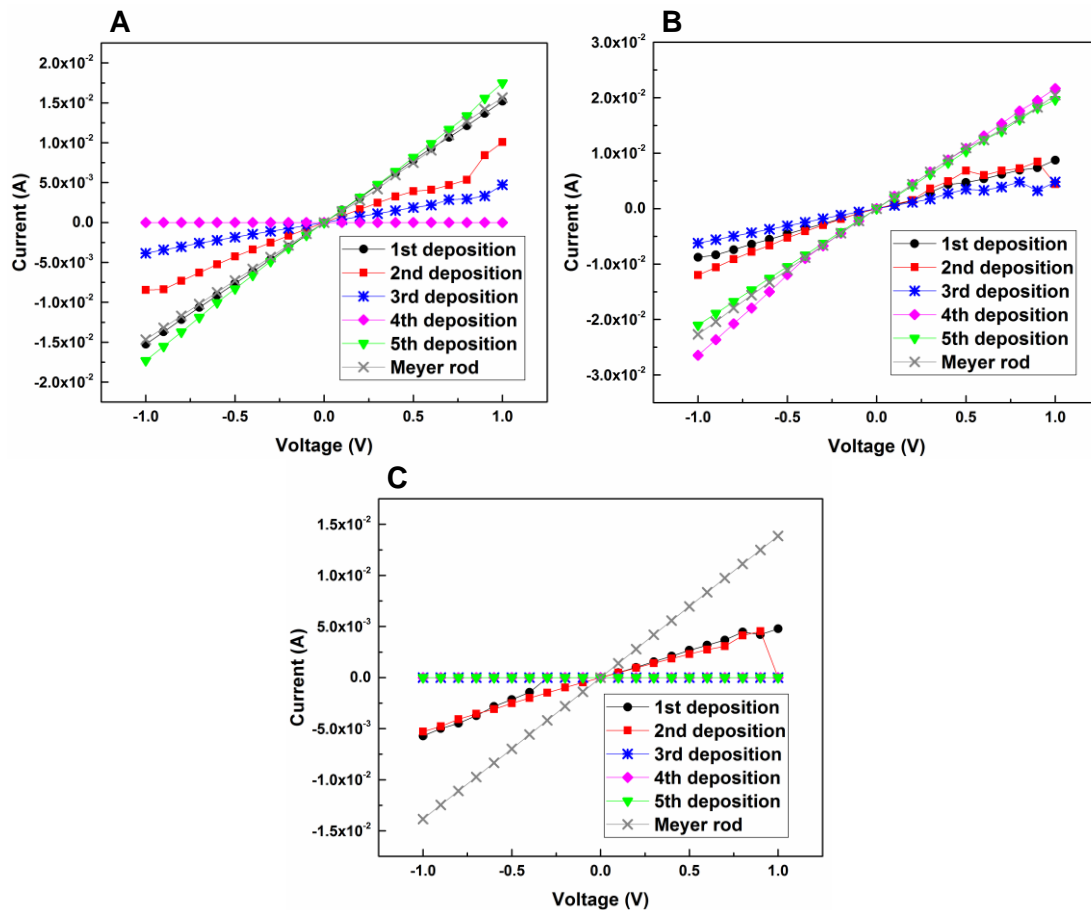
Figure 4.26 – IV curves from several depositions and Meyer rod for several interdigitated contacts gaps, A) has 5 μm, B) has 10 μm and C) has 30 μm.

The interdigitated with spacing of 5 μm were conductive in almost every deposition except from the 4th deposition, which might be due to some undesired particles on the glass surface that could be dragged with the deposition (Figure 4.26 A). Other than that, the highest resistance was 269.54 Ω.

24

Table 4.4 – Resistances calculated for the performed depositions.

Interdigitated's gap	5 μm	10 μm	30 μm
1st deposition	65.10 Ω	108.58 Ω	201.21 Ω
2nd deposition	119.76 Ω	92.34 Ω	207.04 Ω
3rd deposition	269.54 Ω	164.74 Ω	1.6×10^9 Ω
4th deposition	2.65×10^8 Ω	44.00 Ω	1.6×10^8 Ω
5th deposition	60.13 Ω	48.36 Ω	2.8×10^8 Ω
Meyer rod	68.07 Ω	46.19 Ω	71.84 Ω

On the 10 μm spaced interdigitated the resistance was always lower than 200 Ω, however, the ones with higher resistance demonstrated a weird behavior that is not expected from a conductor (Figure 4.26 B). The interdigitated with a gap of 30 μm managed to score a resistance near 200 Ω. Such fact could be due to some long NW given that, as shown before, NWs lengths can reach up to ca. 35 μm (Figure 4.26 C). That same wire maintained its initial position during the second deposition, but eventually it got moved with the other depositions, resulting in a resistance increase. However, with more passages, more NWs are deposited, increasing the possibility of creating a conductive path. The conductive path was established with the Meyer rod, which must have drastically decreased the contact resistance between NWs (Table 4.4). Interestingly, the resistance per gap distance in the first deposition decreased with the gaps' augment. The resistance per gap distance (first deposition) for 5 μm, 10 μm and 30 μm was 13.02 Ω/μm, 10.86 Ω/μm and 6.71 Ω/μm, respectively. However, further studies are required to take conclusions about this behavior, because there are a lot of uncontrolled variables, such as number of NWs between contacts.

Previously the Meyer rod was able to lead to a fully ohmic behavior, and now its usage produced a fully functional contact. These finding point to the fact that the function of the Meyer rod is purely to apply pressure on the NWs.

There is no clear correlation between the number of depositions and resistance of NWs' film.
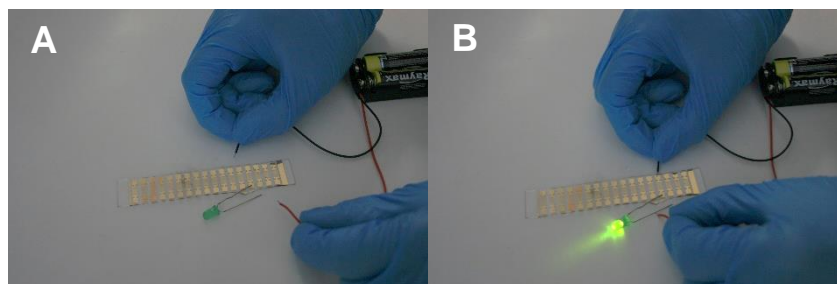
Figure 4.27 – Photographs showing CuNWs on interdigitated contacts as a conductive medium. Image A) shows the LED in off state, and image B) shows the LED in ON state.

Figure 4.27 shows a possible application for CuNWs on interdigitated contacts. Once the needed voltage is supplied to the system (Figure 4.27 B), a LED is turned ON due to the current flowing through the CuNWs, placed between the interdigitated contacts.

4.2.3.1.2. Conductive copper nanowires films

The films created with the same parameters as those pointed out in Chapter 4.2.3.1.1 were not conductive, so the number of depositions was increased to ten, leading to a very dense mesh. Figure 4.28 shows the highly dense mesh with aluminum contacts on top, where the aluminum pads are separated by 160 μm. However, there was no improvement in terms of conduction, which could be due to a high resistance between the NWs. Hence, the NW's film was pressed with a Meyer rod which, nevertheless, produced no improvement. Thus, a piece of glass was placed on top of the film to apply pressure on it, aiming to make it conductive.
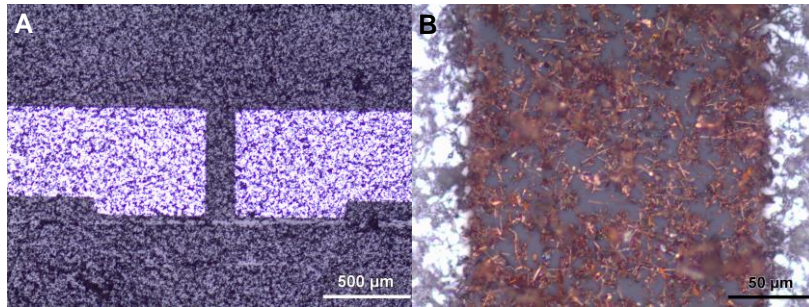
Figure 4.28 – Optical miscroscopy images of a CuNWs' film with aluminum contacts on top. In image A) an overview of the contact is presented, B) shows a close up, where one may to see that the NWs on the contact area are covered with aluminum.

Still no improvement was registered with the suggestion previously made, and some NWs were taken out by the glass that was applying pressure on them.

Consequently, a limited number of adhesion promoters were tested in order to minimize the number of NWs taken out when applying pressure. The options used were silanization by vacuum, silanization by solution (using APTES) and UV treatment. Vacuum silanization and silanization by solution were used because they modify the surface of the glass with fluorin terminates [37] and with amine terminates, respectively [32]. In turn, UV treatment will activate the surface and break some bonds, which might link to the NWs. Firstly, the contact angles were measured between a drop of water and the glass with or without surface treatment, since contact angle is one of the easiest ways to obtain some knowledge about the surface energy. As shown in Figure 4.29, vacuum silanization made the surface hydrophobic, which makes it impossible to use, because the treated surface will not allow a nice spread of the solution of IPA and NWs. APTES makes the surface less hydrophilic, but still able to be covered with the NWs solution. UV treatment makes the surface more hydrophilic.
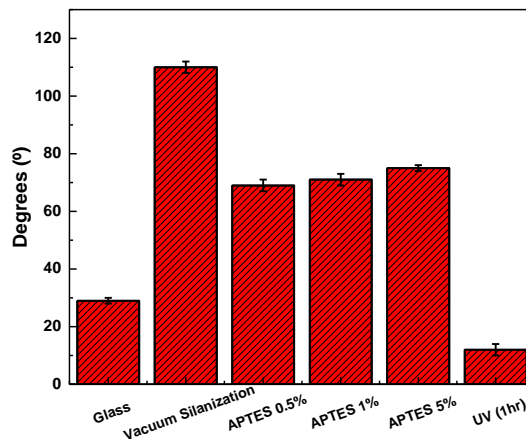
Figure 4.29 – Graphic showing the average contact angles of a water droplet on glass and on all the tested surface treatments.

Since the difference between APTES concentration does not affect much the contact angle, the lowest concentration solution was used from now on.

A glass was treated with APTES 0.5 % and five depositions were done after the treatment. The result can be seen in the following image Figure 4.30.
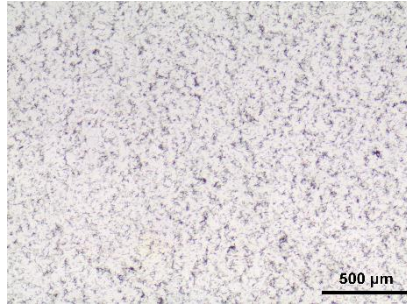
Figure 4.30 – Optical microscopy image of the results of a glass treated with APTES 0.5 %, followed five depositions.

The NWs' net did not seem to be able to conduct, which may be attributed to the many spots free of NWs. So, a new glass was treated with the same APTES solution, but this time, after the treatment, ten depositions were applied to it.
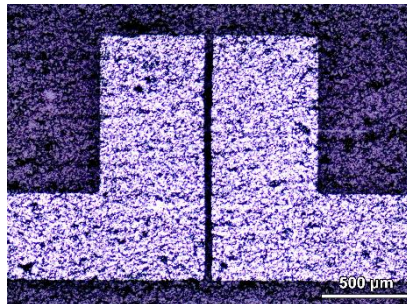
Figure 4.31 – Optical microscopy image of the same film presented in Figure 4.30, with aluminum contacts on top.

However, since the contacts were deposited by e-beam, which is a very vertical type of deposition, the roughness of the film was able to make the contacts not conductive. The masks for the deposition of contacts have a circle that is used to check the contacts quality. So, one of those circles was used to measure the roughness of the film. The contact used did not have NWs in the middle, and the NWs around the contact were cleaned, to make sure they would not be drafted by the profilometer's tip (Figure 4.32).
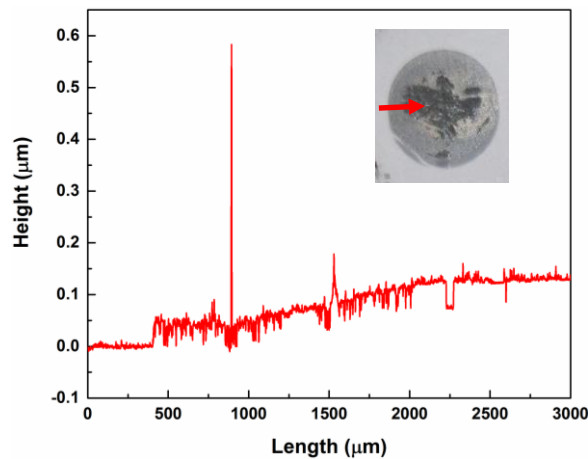
Figure 4.32 – Graphic showing the profile of an aluminum contact deposited on top of NWs. Inset shows the contact and the direction of the scanning.

The deposition of aluminum reached 100 nm, but it was not constant throughout the circle, and the roughness of the film is clearly excessive.

Another option is bottom contacts. However, in that case the surface treatment cannot be applied, since it would deposit amine terminates on the contacts.

27

4.2.3.2. Optical characterization

In the electrical characterization of the NWs deposited on interdigitated's contacts, no correlation between the number of depositions and the resistance was found. However, since there are more NWs deposited after each deposition, the optical properties might change at every deposition. So, five substrates were prepared, each one with an increasing number of passages (Figure 4.33).
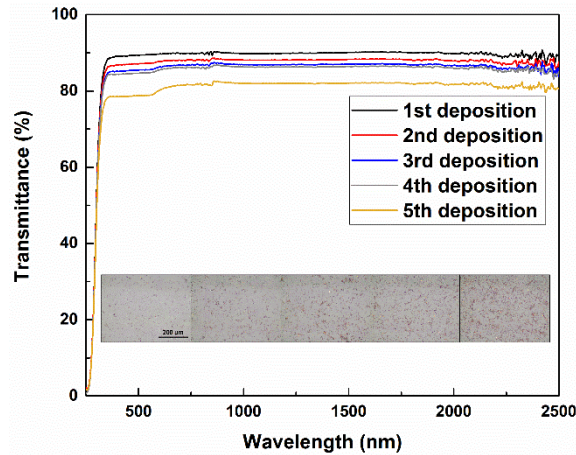
Figure 4.33 – Graphic showing the transmittance versus wavelength for all five depositions. Inset show microscopic images from the 5 substrates.

The films demonstrated a good performance overall and quite persistent behavior throughout the solar spectrum.
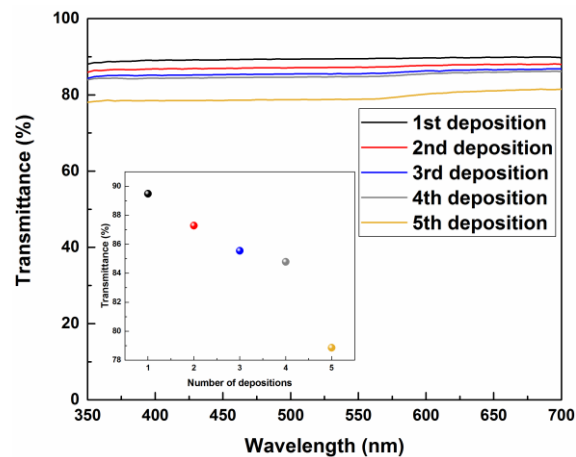
Figure 4.34 – Graphic showing the transmittance versus wavelength at the visible spectrum for the five depositions. Inset shows the transmittance at 550 nm for all the depositions.

The transmittance decayed with the number of depositions, almost in a linear way, which represents, albeit not very accurately, that the number of NWs deposited each time is similar (Figure 4.34).

28

5.   CONCLUSIONS AND FUTURE PERSPECTIVES

In this work, NWs were produced via chemical reaction mediated by EDA. Two methods were used, one with copper acetate and another one with copper nitrate. The NWs produced with copper acetate were deposited on glass substrates and on gold interdigitated through several deposition methods, in order to create films of CuNWs. These films were characterized electrically and optically.

5.1.   Final conclusions

CuNWs were synthesized via chemical reaction mediated by EDA. First copper acetate was used. In the standard copper acetate synthesis tested herein, CuNWs had a diameter of about 250 nm and lengths of around 11 µm. Doubling the amount of EDA added to the synthesis made CuNWs thinner by ca. 83 nm and it also increased the average length by almost 1 µm. However, it also increased the relative frequency of CuNWs with sizes between 0 µm and 5 µm. Augmenting the presence of hydrazine in the solution led to the formation of clusters on the CuNWs, which makes them inviable to usage. Leaving the CuNWs in the solution for one more hour did not exhibit any significant difference. Then CuNWs were produced using copper nitrate. In this synthesis a supernatant is formed after 15 minutes, however it needs to mature for 45 minutes, leading to a water bath 60 minutes long. The average length of this NWs was 19.6 ± 12.5 µm, with some wires reaching more than 65 µm.

Table 5.1 – Summary of the prices for a synthesis of CuNWs using copper acetate.

Reagent	Quantity	Price (€)	Price per synthesis × 10^{-3} (€)
Copper(II) acetate	25 g	268	493.1
EDA (99%)	1 L	73.4	3.7
Hydrazine (65%)	500 g	43	0.9
NaOH	1 kg	153.7	3688.8
Total	-	-	4186.5

Table 5.2 – Summary of the prices for a synthesis of CuNWs using copper nitrate.

Reagent	Quantity	Price (€)	Price per synthesis × 10^{-3} (€)
Copper(II) nitrate	250 g	304.5	113.3
EDA (75-80%)	1 L	41.5	24.9
Hydrazine (65%)	500 g	43	4.4
NaOH	1 kg	153.7	3688.8
Total	-	-	3831.5

From Table 5.1 and Table 5.2 one concludes that the synthesis using copper nitrate is cheaper than the one using copper acetate. Though copper nitrate and copper acetate have a big difference in prices, the final price per synthesis comes very close, because the greatest expense is due to NaOH. With the increased number of reactions, it becomes clear that both synthesis price will be controlled by NaOH. Nevertheless, a synthesis of CuNWs using copper nitrate costs less than 4 €.

The synthesized CuNWs with copper acetate were then used to create films by three different deposition methods: drop casting, spray coating, and doctor blade. Drop casting main problems were

the formation of coffee rings and some aggregation. Spray coating did not deposit CuNWs in a uniform way and also generated aggregates, which matches some results available on the literature [24]. Doctor blade showed the most promising results. Firstly, a Meyer rod was used, and due to the difficulty of depositing a sufficient number of CuNWs to get a conductive film, some solutions were tested. Nevertheless, the used solutions did not demonstrate the desired results. So, a new method was developed. This new method exhibited promising results and created conductive films on top of gold interdigitated.

Unfortunately, no conductive films were achieved and two major problems arose: CuNWs poor adhesion to the substrate and surface roughness. The first difficulty was tackled with surface treatments, in which APTES demonstrated some promising results. However, this strategy adds some problems to the usage of bottom contacts. Surface roughness did not allow for the use of top contacts, so further investigation must be done.

The deposited films exhibited a good performance throughout the solar spectrum and transmittance decayed in an almost linear way.

Best balance in terms of electrical/optical properties was achieved with a single deposition, for which R = 65 Ω (5 µm gap) and %T = 90 were obtained.

Considering a two inch's ITO sputtering target that is able to deposit contacts with 10×10 cm^2 for 100 depositions, this will cost 0.1 €/cm^2. A copper synthesis will cost ca. 0.004 €/cm^2. It is worth to notice that both prices will increase considering machinery price, but that will increase the difference between both methods, making CuNWs much worthier to use.

5.2.   Future perspectives

This work showed very promising results in an embryonic branch of studies at CENIMAT. Combining both the synthesis study and the advances on deposition methods, conductive films will be achieved in the near future. Nevertheless, there is plenty of work to do.

One of the first things do is to characterize electrically and optically the CuNWs produced with copper nitrate, since this will lead to much cheaper transparent contacts.

In the deposition methods, further studies can be performed with spray coating to fully understand its possibility of usage. In doctor blade, a film applicator with less speed of deposition would allow the introduction of some studies with the droplet behavior. This effect might induce some order to the NWs network and an ordered net has the potential to augment optical transmittance.

The low adhesion of the NWs to glass can be overtaken by changing the substrate. Polymers are very interesting options, because they allow applications where bending or stretching is required.

Surface roughness is a very important point, since it can make a contact unusable on LEDs or PVs. LEDs and PVs demand for contacts with low surface roughness mainly due to spikes that generate leakage currents. Covering the NWs film or embedding the NWs with a new material can reduce the surface roughness and it can also augment the NWs resistance to oxidation. Another way to reduce oxidation is by depositing the NWs in some guiding lines with a depth related to the NWs' diameter.

The stability of CuNWs on interdigitated or functional CuNWs films at different temperatures should also be implemented, since temperature makes the wires more prone to oxidation. Also, in applications like displays, temperatures can raise substantially.

6. BIBLIOGRAPHY

[1] P.-C. Hsu, S. Wang, H. Wu, V. K. Narasimhan, D. Kong, H. Ryoung Lee, and Y. Cui, "Performance enhancement of metal nanowire transparent conducting electrodes by mesoscale metal wires.," *Nat. Commun.*, vol. 4, p. 2522, 2013. doi: http://dx.doi.org/10.1038/ncomms3522

[2] S. Ye, A. R. Rathmell, I. E. Stewart, Y.-C. Ha, A. R. Wilson, Z. Chen, and B. J. Wiley, "A rapid synthesis of high aspect ratio copper nanowires for high-performance transparent conducting films," *Chem. Commun.*, vol. 50, no. 20, pp. 2562–2564, 2014. doi: http://dx.doi.org/10.1039/C3CC48561G

[3] Z. Chen, S. Ye, I. E. Stewart, and B. J. Wiley, "Copper nanowire networks with transparent oxide shells that prevent oxidation without reducing transmittance," *ACS Nano*, vol. 8, no. 9, pp. 9673–9679, 2014. doi: http://dx.doi.org/10.1021/nn504308n

[4] R. G. Gordon, "Criteria for Choosing Transparent Conductors," *MRS Bull.*, vol. 25, no. 8, pp. 52–57, 2000. doi: http://dx.doi.org/10.1557/mrs2000.151

[5] A. R. Rathmell, S. M. Bergin, Y. L. Hua, Z. Y. Li, and B. J. Wiley, "The growth mechanism of copper nanowires and their properties in flexible, transparent conducting films," *Adv. Mater.*, vol. 22, no. 32, pp. 3558–3563, 2010. doi: http://dx.doi.org/10.1002/adma.201000775

[6] C. H. Chung, T. Bin Song, B. Bob, R. Zhu, and Y. Yang, "Solution-processed flexible transparent conductors composed of silver nanowire networks embedded in indium tin oxide nanoparticle matrices," *Nano Res.*, vol. 5, no. 11, pp. 805–814, 2012. doi: http://dx.doi.org/10.1007/s12274-012-0264-8

[7] D. Langley, G. Giusti, C. Mayousse, C. Celle, D. Bellet, and J. P. Simonato, "Flexible transparent conductive materials based on silver nanowire networks: a review," *Nanotechnology*, vol. 24, no. 45, p. 452001, 2013. doi: http://dx.doi.org/10.1088/0957-4484/24/45/452001

[8] H. Guo, N. Lin, Y. Chen, Z. Wang, Q. Xie, T. Zheng, N. Gao, S. Li, J. Kang, D. Cai, and D.-L. Peng, "Copper nanowires as fully transparent conductive electrodes.," *Sci. Rep.*, vol. 3, p. 2323, 2013. doi: http://dx.doi.org/10.1038/srep02323

[9] L. Hu, H. Wu, and Y. Cui, "Metal nanogrids, nanowires, and nanofibers for transparent electrodes," *MRS Bull.*, vol. 36, no. 10, pp. 760–765, 2011. doi: http://dx.doi.org/10.1557/mrs.2011.234

[10] S. Chen, L. Brown, M. Levendorf, W. Cai, S. Y. Ju, J. Edgeworth, X. Li, C. W. Magnuson, A. Velamakanni, R. D. Piner, J. Kang, J. Park, and R. S. Ruoff, "Oxidation resistance of graphene-coated Cu and Cu/Ni alloy," *ACS Nano*, vol. 5, no. 2, pp. 1321–1327, 2011. doi: http://dx.doi.org/10.1021/nn103028d

[11] L. Hu, H. S. Kim, J. Lee, P. Peumans, and Y. Cui, "Scalable Coating and Properties of transparent Ag nanowire," *ACS Nano*, vol. 4, no. 5, pp. 2955–2963, 2010. doi: http://dx.doi.org/10.1021/nn1005232

[12] C. F. Guo and Z. Ren, "Flexible transparent conductors based on metal nanowire networks," *Mater. Today*, vol. 18, no. 3, pp. 143–154, 2015. doi: http://dx.doi.org/10.1016/j.mattod.2014.08.018

[13] Encyclopædia Britannica Online, "Metal." [Online]. Available: https://www.britannica.com/science/metal-chemistry. [Accessed: 15-Aug-2016].

[14] S. Han, S. Hong, J. Yeo, D. Kim, B. Kang, M. Y. Yang, and S. H. Ko, "Nanorecycling: Monolithic Integration of Copper and Copper Oxide Nanowire Network Electrode through Selective Reversible Photothermochemical Reduction," *Adv. Mater.*, vol. 27, no. 41, pp. 6397–6403, 2015. doi: http://dx.doi.org/10.1002/adma.201503244

[15] A. R. Rathmell, M. Nguyen, M. Chi, and B. J. Wiley, "Synthesis of oxidation-resistant cupronickel nanowires for transparent conducting nanowire networks," *Nano Lett.*, vol. 12, no. 6, pp. 3193–3199, 2012. doi: http://dx.doi.org/10.1021/nl301168r

[16]   P. Lee, J. Lee, H. Lee, J. Yeo, S. Hong, K. H. Nam, D. Lee, S. S. Lee, and S. H. Ko, "Highly stretchable and highly conductive metal electrode by very long metal nanowire percolation network," *Adv. Mater.*, vol. 24, no. 25, pp. 3326–3332, 2012. doi: http://dx.doi.org/10.1002/adma.201200359

[17]   Encyclopædia Britannica Online, "Copper (Cu)." [Online]. Available: https://www.britannica.com/science/copper. [Accessed: 15-Aug-2016].

[18]   N. N. Greenwood and A. Earnshaw, *Chemistry of the Elements*. Elsevier Science, 2012.

[19]   R. L. Graham, G. B. Alers, T. Mountsier, N. Shamma, S. Dhuey, S. Cabrini, R. H. Geiss, D. T. Read, and S. Peddeti, "Resistivity dominated by surface scattering in sub-50 nm Cu wires," *Appl. Phys. Lett.*, vol. 96, no. 4, pp. 33–36, 2010. doi: http://dx.doi.org/10.1063/1.3292022

[20]   Y. Chang, M. L. Lye, and H. C. Zeng, "Large-scale synthesis of high-quality ultralong copper nanowires.," *Langmuir*, vol. 21, no. 9, pp. 3746–8, Apr. 2005. doi: http://dx.doi.org/10.1021/la050220w

[21]   Y. Shi, H. Li, L. Chen, and X. Huang, "Obtaining ultra-long copper nanowires via a hydrothermal process," *Sci. Technol. Adv. Mater.*, vol. 6, no. 7, pp. 761–765, Oct. 2005. doi: http://dx.doi.org/10.1016/j.stam.2005.06.008

[22]   D. Zhang, R. Wang, M. Wen, D. Weng, X. Cui, J. Sun, H. Li, and Y. Lu, "Synthesis of ultralong copper nanowires for high-performance transparent electrodes," *J. Am. Chem. Soc.*, vol. 134, no. 35, pp. 14283–14286, 2012. doi: http://dx.doi.org/10.1021/ja3050184

[23]   S. Ye, I. E. Stewart, Z. Chen, B. Li, A. R. Rathmell, and B. J. Wiley, "How Copper Nanowires Grow and How to Control Their Properties," *Acc. Chem. Res.*, vol. 49, no. 3, pp. 442–451, 2016. doi: http://dx.doi.org/10.1021/acs.accounts.5b00506

[24]   A. R. Rathmell and B. J. Wiley, "The synthesis and coating of long, thin copper nanowires to make flexible, transparent conducting films on plastic substrates," *Adv. Mater.*, vol. 23, no. 41, pp. 4798–4803, 2011. doi: http://dx.doi.org/10.1002/adma.201102284

[25]   J. Chen, W. Zhou, J. Chen, Y. Fan, Z. Zhang, Z. Huang, X. Feng, B. Mi, Y. Ma, and W. Huang, "Solution-processed copper nanowire flexible transparent electrodes with PEDOT:PSS as binder, protector and oxide-layer scavenger for polymer solar cells," *Nano Res.*, vol. 8, no. 3, pp. 1017–1025, 2015. doi: http://dx.doi.org/10.1007/s12274-014-0583-z

[26]   D. Nunes, A. Pimentel, P. Barquinha, P. a. Carvalho, E. Fortunato, and R. Martins, "Cu$_2$O polyhedral nanowires produced by microwave irradiation," *J. Mater. Chem. C*, vol. 2, pp. 6097–6103, 2014. doi: http://dx.doi.org/10.1039/c4tc00747f

[27]   W. Hu, X. Niu, L. Li, S. Yun, Z. Yu, and Q. Pei, "Intrinsically stretchable transparent electrodes based on silver-nanowire–crosslinked-polyacrylate composites," *Nanotechnology*, vol. 23, no. 34, p. 344002, 2012. doi: http://dx.doi.org/10.1088/0957-4484/23/34/344002

[28]   F. Xu and Y. Zhu, "Highly conductive and stretchable silver nanowire conductors," *Adv. Mater.*, vol. 24, no. 37, pp. 5117–5122, 2012. doi: http://dx.doi.org/10.1002/adma.201201886

[29]   Z. Zhu, T. Mankowski, K. Balakrishnan, A. S. Shikoh, F. Touati, M. A. Benammar, M. Mansuripur, and C. M. Falco, "Ultrahigh Aspect Ratio Copper-Nanowire-Based Hybrid Transparent Conductive Electrodes with PEDOT:PSS and Reduced Graphene Oxide Exhibiting Reduced Surface Roughness and Improved Stability.," *ACS Appl. Mater. Interfaces*, vol. 7, no. 30, pp. 16223–30, 2015. doi: http://dx.doi.org/10.1021/acsami.5b01379

[30]   C. Celle, C. Mayousse, E. Moreau, H. Basti, A. Carella, and J. P. Simonato, "Highly flexible transparent film heaters based on random networks of silver nanowires," *Nano Res.*, vol. 5, no. 6, pp. 427–433, 2012. doi: http://dx.doi.org/10.1007/s12274-012-0225-2

[31]   V. Scardaci, R. Coull, P. E. Lyons, D. Rickard, and J. N. Coleman, "Spray deposition of highly transparent, low-resistance networks of silver nanowires over large areas," *Small*, vol. 7, no. 18, pp. 2621–2628, 2011. doi: http://dx.doi.org/10.1002/smll.201100647

[32]   S. Kang, T. Kim, S. Cho, Y. Lee, A. Choe, B. Walker, S. J. Ko, J. Y. Kim, and H. Ko, "Capillary printing of highly aligned silver nanowire transparent electrodes for high-performance optoelectronic devices," *Nano Lett.*, vol. 15, no. 12, pp. 7933–7942, 2015. doi: http://dx.doi.org/10.1021/acs.nanolett.5b03019

[33]   J. Y. Lee, S. T. Connor, Y. Cui, and P. Peumans, "Solution-processed metal nanowire mesh transparent electrodes," *Nano Lett.*, vol. 8, no. 2, pp. 689–692, 2008. doi: http://dx.doi.org/10.1021/nl073296g

[34]   S. Han, S. Hong, J. Ham, J. Yeo, J. Lee, B. Kang, P. Lee, J. Kwon, S. S. Lee, M. Y. Yang, and S. H. Ko, "Fast plasmonic laser nanowelding for a cu-nanowire percolation network for flexible transparent conductors and stretchable electronics," *Adv. Mater.*, pp. 1–7, 2014. doi: http://dx.doi.org/10.1002/adma.201400474

[35]   I. E. Stewart, A. R. Rathmell, L. Yan, S. Ye, P. F. Flowers, W. You, and B. J. Wiley, "Solution-processed copper-nickel nanowire anodes for organic solar cells," *Nanoscale*, vol. 6, no. 11, pp. 5980–5988, 2014. doi: http://dx.doi.org/10.1039/C4NR01024H

[36]   C. Sachse, N. Weiß, N. Gaponik, L. Müller-Meskamp, A. Eychmüller, and K. Leo, "ITO-Free, Small-Molecule Organic Solar Cells on Spray-Coated Copper-Nanowire-Based Transparent Electrodes," *Adv. Energy Mater.*, vol. 4, no. 2, p. 1300737, Jan. 2014. doi: http://dx.doi.org/10.1002/aenm.201300737

[37]   V. Sunkara, D.-K. Park, H. Hwang, R. Chantiwas, S. A. Soper, and Y.-K. Cho, "Simple room temperature bonding of thermoplastics and poly(dimethylsiloxane).," *Lab Chip*, vol. 11, no. 5, pp. 962–965, 2011. doi: http://dx.doi.org/10.1039/c0lc00272k
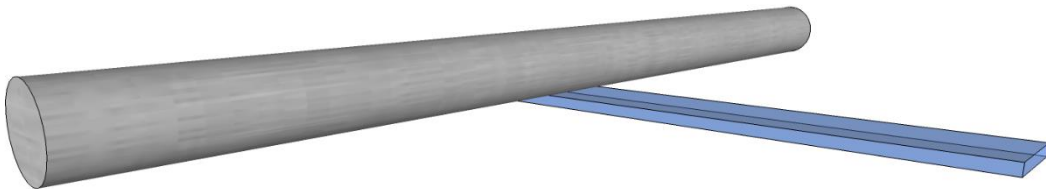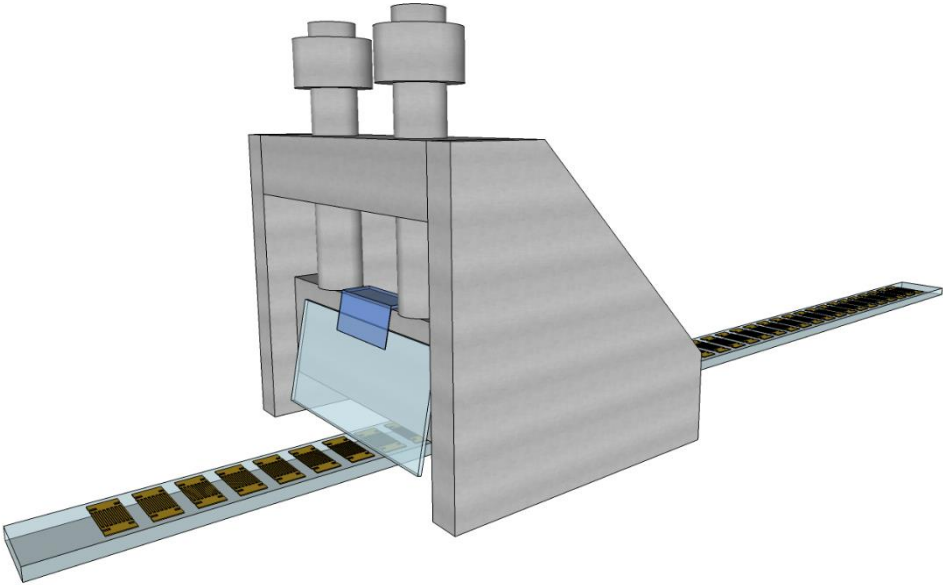
7. ANNEX

Annex A – Schematic of drop casting method A) without temperature and B) with temperature.
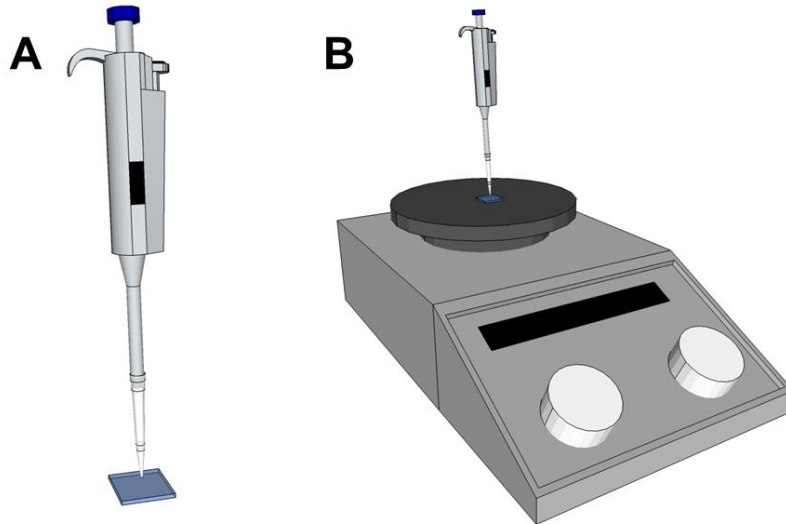
Annex B – Schematic of the meyer rod deposition method.

Annex C – Schematic of the newly designed method.

Annex D – Schematic of the interdigitated contacts array used.